



NTNU – Trondheim
Norwegian University of
Science and Technology

Modeling of Reaction Calorimeter

Reza Farzad

Chemical Engineering

Submission date: June 2014

Supervisor: Hanna Knuutila, IKP

Norwegian University of Science and Technology
Department of Chemical Engineering

Preface:

This master thesis completes my two-year master studies in Chemical Engineering at Norwegian University of Science and Technology. During these two years, I have found many decent friends and teachers who have helped me to learn and experience new subjects, and I have a lot of good memories with them.

I would like to say my special thanks to my supervisor, Hanna Knuutila associated professor at chemical engineering department who gave me a lot of trust and academic supports during my project. I am also thankful to my co-supervisor professor Hallvard Fjøsne Svendsen because of his useful advices.

I would thank Diego Pinto, for helping me in solving my problem during the project. Also, I would like to express my thanks to Inna Kim, Anastasia Alexandrovna Trollebø, Ardi Hartono, Gøril Flatberg and all of my friends who have helped me during this project in different ways.

Finally, I am very grateful to my parents who have always supported me during my life, and I would like to dedicate my thesis to them.

I declare that this is an independent work according to the exam regulations of the Norwegian University of Science and Technology.

Trondheim, 17 June 2014

Reza Farzad

Abstract:

The purpose of this project was to model the reaction calorimeter in order to calculate the heat of absorption which is the most important parameter in this work. Reaction calorimeter is an apparatus which is used in measuring the heat of absorption of CO₂ as well as the total pressure in vapor phase based on vapor-liquid equilibrium state. Mixture of monoethanolamine (MEA) and water was used as a solvent to absorb the CO₂. Project was divided in to three parts in order to make the programming procedure easier. Also, the entire programming in this project was implemented in MATLAB®. These parts are: vapor-liquid equilibrium calculation, loading calculation and calculation of heat of absorption. Vapor-liquid equilibrium calculation was based on the eNRTL model. Total pressure and partial pressure of CO₂ which were calculated by this part for 30% MEA solution at 40 °C, 80 °C and 120 °C were plotted against loading and the results are fairly close to the experimental data and validated vapor-liquid equilibrium model to be used for the rest of the project. Loading calculation was the next part of the project, the new loadings were calculated based on the injected amount of CO₂ in to the reaction calorimeter. Total pressure and partial pressure of CO₂ were computed based on the new loading and the results were plotted against the calculated loadings for 30% MEA solution at 40 °C, 80 °C and 120 °C. For these three temperatures, results from the written model and experimental data had the same trend. The last objective of this project was to calculate the heat of absorption, which is the main concern in chemical industries, to provide enough energy to separate CO₂ from solvent solution in the solvent recovery unit. Developed model for this part could predict overall heat of absorption. Comparison between the obtained results from this model and the model developed by Kim et al. (Kim et al., 2009) and experimental data were satisfying. Since the results were quite acceptable in comparison to experimental data, this written model might be good to describe the reaction calorimeter in order to meet the goal of this project.

Table of contents:

Preface:	I
Abstract:	II
Table of contents:	III
Nomenclature:	V
1. Introduction:	1
1.1 Carbon capture and storage:	1
1.1.1 Capture from industrial process streams:	1
1.1.2 Post-combustion capture:	2
1.1.3 Oxy-Fuel combustion capture:	2
1.1.4 Pre-combustion capture:	2
1.1.5 CO ₂ storage:	2
1.2 CO ₂ absorption process:	3
1.3 Heat of absorption	4
1.4 Scope of work.....	5
2. Thermodynamic background:	6
2.1 Vapor-liquid equilibrium:	6
2.1.1 The chemical potential:	8
2.1.2 Fugacity and fugacity coefficient:	9
2.1.3 Activity and activity coefficient:	10
2.1.4 $\phi - \phi$ Method:	11
2.1.5 $\gamma - \phi$ Method:	11
2.2 Chemical Equilibria:	12
2.2.1 Chemical equilibria constant:	12
2.2.2 Effect of temperature on the equilibrium constant:	13
2.3 Heat of absorption:	14
2.4 Electrolyte Non-Random Two-Liquid (eNRTL) model:.....	15
3. Modeling of reaction calorimeter:	18
3.1 Reaction calorimeter apparatus:	18
3.2 Code development:.....	20
3.2.1 Loading calculation:	20
3.2.2 Heat of absorption:	25
4. Results and Discussion:	28

4.1 Vapor-liquid equilibrium model verification:.....	28
4.2 Loading calculation:	30
4.3 Heat of absorption:	35
5. Conclusion:	42
5.1 Future work:	42
Bibliography:	43
Appendix A:	46
Appendix B:	57

Nomenclature:

Latin letters:

A	chemical formula [-]
a	activity [-]
A,B,C,D	constants [-]
f	fugacity [KPa]
G	gibbs energy [KJ/mol]
H	enthalpy [KJ]
<i>H</i>	henry's law constant [KPa]
K	equilibrium constant [-]
n	number of moles [-]
P	pressure [KPa]
Q	heat [KJ]
R	universal gas constant [8.314e-3 KJ/mol K]
S	entropy [KJ/K]
T	temperature [K]
U	internal energy [KJ]
V	volume [m ³]
W	work [KJ]
x	mole fraction-liquid phase [-]
y	mole fraction-vapor phase [-]
z	charge number [-]

Greek letters:

α	loading [mol CO ₂ /mol MEA]
α	symmetric nonrandom factor parameters [-]
γ	acidity coefficient [-]
ζ	extents of reaction [-]
μ	chemical potential, viscosity [Pa s]
ν	stoichiometric coefficient [-]
ρ	density [Kg/m ³]
φ	fugacity coefficient [-]

v

Subscripts:

a	anionic segment species
c	cationic segment species
i	species i
I,J	component species
i,j,k	segment-based species
lc	local composition
m	molecular segment species
rev	reversible process

Superscripts:

0	Standard state
E	excess
L	liquid phase
sat	saturation
V	vapor phase

Abbreviation:

CCS	carbon capture and storage
eNRTL	electrolyte non-random two liquid
MEA	mono-ethanol-amine
STP	standard temperature and pressure
VLE	vapor-liquid equilibrium

1. Introduction:

Today's energy market trends are eventually changing in the world. Most of the energy importer and exporter countries are switching their places with each other. China, India and Middle East countries are quickly becoming the world largest energy consumers. China and India will be the largest importer of the oil and coal by the 2020s, respectively. Energy industries are the main source of greenhouse-gases by having two-thirds of the world total emission, and they play the leading role in climate-change issue. (Biol, 2004).

1.1 Carbon capture and storage:

Nowadays, Carbon capture and storage (CCS) is the main process in removing the CO₂ from industrial reactions and keeping it away from entering the atmosphere by storing CO₂ in geological formation. This method can eliminate around 85%-95% of CO₂ which is produced in an industrial plant. High energy consumption is the primary issue of this process. For instance a power plant with CCS system requires 10-40% more energy compared to a plant without CCS system. In other hand, a plant with CCS system is able to eliminate 80%-90% CO₂ compared to a plant without CCS (Metz et al., 2005)

Four fundamental types for CO₂ capture from the chemical industry and power stations are shown as below:

- Capture from industrial process streams
- Post-combustion capture
- Oxy-fuel combustion capture
- Pre-combustion capture

1.1.1. Capture from industrial process streams:

During the last 80 years, CO₂ has been removed from industrial process streams(Kohl and Nielsen, 1997) but main part of the CO₂ is sent to the atmosphere since storage is not demanded. Also, Post-combustion, Oxy-Fuel combustion capture and Pre-combustion capture are popular methods in order to capture the CO₂ from industrial process streams.

1.1.2 Post-combustion capture:

Combusted fossil fuels and biomasses in the air form flue gases. Elimination of CO₂ from these flue gases is called “Post-combustion capture”. In this method, flue gas is sent to scrubber and cooled down with water spray initially, then it goes to the absorber where the lean amine solvent captures CO₂ and becomes rich solvent. Then rich solvent is treated in stripper column by heating up. Finally lean solvent is recycled back to the process from the bottom and CO₂ vents from the top section of stripper column(Wang et al., 2011).

1.1.3 Oxy-Fuel combustion capture:

In this system, oxygen is applied instead of air in combustion process. Combusted fuel and pure oxygen leads to a flue gas which mostly contains CO₂ and H₂O. Flue gas does not need to be treated and remaining H₂O can be condensed from flue gas(Oki et al., 2011). Moreover, flue gas can be used as a recycle to combustor in order to adjust the temperature since combustion with pure oxygen produces an extremely high temperature. Cryogenic air separation is required to produce pure oxygen.

1.1.4 Pre-combustion capture:

Steam reforming is the main process in this method where reaction of fuel and oxygen/air with steam produces synthesis gas (CO+H₂). Then, CO is reacted with H₂O and converted to CO₂ and more H₂ by a catalytic reactor (shift reactor). CO₂ is removed from the stream and then only H₂ remains in the stream. H₂ can be used as a fuel for different application(Kanniche et al., 2010). This process is known as Pre-combustion capture.

1.1.5 CO₂ storage:

CO₂ can be stored in empty oil and gas reservoirs deep saline aquifers or unmineable coal seams (Gluyas and Mathias, 2013). Compressed CO₂ (compacted into 0.2% of its Volume at STP) can be carried via pipelines, ships or trucks(Skovholt, 1993). Also, some countries are trying to calculate how much CO₂ they can store and if this amount can have influence on CO₂ reduction from atmosphere (Gluyas and Mathias, 2013).

1.2 CO₂ absorption process:

The main absorption process consists of two packed columns, which are known as absorber and desorber (stripper) columns. First, flue gas is cooled to lower temperature. Then, cold flue gas enters to the absorber column from bottom and the liquid solvent drips from top side of the column to down in a countercurrent form. This liquid includes reactive chemical species, which is improving CO₂ solubility in the liquid. After that, Rich solvent (liquid solvent and absorbed CO₂) goes to desorber column, which is working at higher temperature and the solvent drips from top side to bottom of the column. Steam from desorber column's reboiler has enough energy to remove CO₂ from rich solvent and vent out the CO₂ from top side. On the other hand, high-energy requirement in the reboiler to produce steam, which has enough energy in order to strip CO₂ from solvent is a big concern. Finally, the treated solvent is sent to the absorber column as a lean solvent. These procedures are occurring continuously. Figure 1.1 indicates CO₂ absorption process.

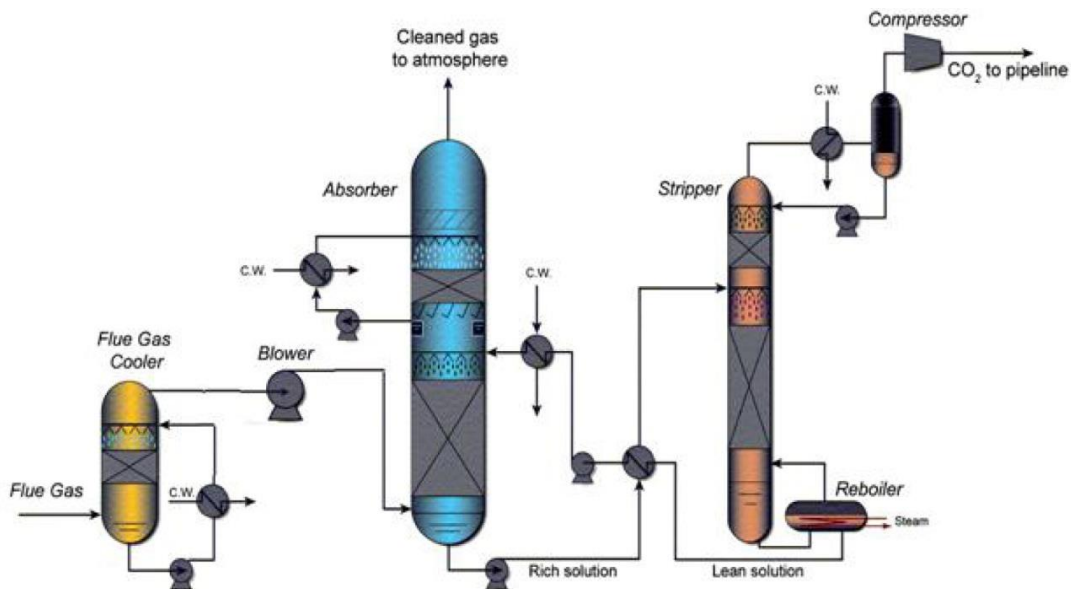


Figure 1.1: CO₂ absorption process (Tobiesen A.F, 2006)

CO₂ absorption solvent should be a mixture with high reaction rate, high stability and low vapor pressure. Nowadays, Alkanoamines is the most common solvent in CO₂ capture process(Kim, 2009).

1.3 Heat of absorption

Because of the energy cost, heat of absorption could be the most important factor. This energy is required to separate CO₂ from solvent in the regeneration section. Heat of absorption can be calculated from the chemical reactions which are happening during the process, based on thermodynamic rules. Chemical reactions involved in CO₂ absorption by Amine are written as below (Austgen et al., 1989):

Dissociation of water:



Dissociation of carbon dioxide:



Dissociation of bicarbonate:



Dissociation of protonated amine:



Carbamate reversion to bicarbonate:



Physical dissolution of carbon dioxide:



1.4 Scope of work

The main objective of this report is the modeling of a reaction calorimeter which comes in the further chapter in detail. MEA is used in this project as a solvent to capture the CO₂. Modeling part is divided into different parts in order to make the procedure easier. Also, all of these parts are implemented in MATLAB. These parts are:

- Vapor-Liquid equilibrium calculation
- Loading calculation
- Heat of absorption

This project is based on vapor-liquid equilibrium (VLE), since other parts of modeling are depend on it. VLE method consists of fundamental thermodynamic rules which calculate partial pressure of spices in vapor phase and mole fraction of components in liquid phase. Because of implementation complexity this part of project was done by Diego Pinto, PhD student at chemical engineering department of Norwegian University of Science and Technology.

2. Thermodynamic background:

Vapor-liquid equilibrium and heat of absorption which have been implemented in this work are written in this chapter.

In-house codes are written by Diego Pinto are based on vapor-liquid equilibrium thermodynamic. Different thermodynamic equations are required to introduce vapor and liquid phases. Also, number of moles of components related to the equation (1.1) till equation (1.6) are calculated based on the chemical equilibria. Chemical equilibria is based on the Gibbs energy, since system tries to reach equilibrium by minimizing the Gibbs energy. According to equation (1.1) till equation (1.6), following components are available in the liquid phase: H_2O , CO_2 , MEA , H_3O^+ , MEA^+ , OH^- , HCO_3^- , CO_3^{2-} and MEACOO^{2-} . Moreover, H_2O , CO_2 and MEA are presented in vapor phase. One of the most important parameters is the activity coefficient γ which is needed in the liquid phase to introduce the deviation from the ideal liquid mixture. This coefficient is calculated from eNRTL equation (thermodynamic information about eNRTL is given in the further part). Furthermore, partial pressure of species in the vapor phase and mole fraction of the components in liquid phase are calculated in this code.

2.1 Vapor-liquid equilibrium:

A static state without change in the properties in macroscopic scale is called equilibrium. Vapor and liquid phases in an isolated system with close contact finally gain a final state and there is no desire to change the system in macroscopic scale is called vapor-liquid equilibrium. Vapor-liquid calculation is based on the Gibbs energy, since Gibbs energy is minimized when the system approaches an equilibrium state at constant pressure and temperature.

The internal energy for n moles in a closed system is written as below (Smith et al., 2005):

$$d(nU) = dQ_{rev} + dW_{rev} \quad (2.1)$$

Where dQ_{rev} (heat) and dW_{rev} (Work) are:

$$dQ_{rev} = -P d(nV) \quad (2.2)$$

$$dW_{rev} = T d(nS) \quad (2.3)$$

Where P, T, V and S are pressure, temperature, volume and entropy respectively.

Combination of these three equations gives:

$$d(nU) = -P d(nV) + T d(nS) \quad (2.4)$$

As it can be seen, all of the main thermodynamic properties such as P, V, T, U and S are presented in equation (2.4). Furthermore, Enthalpy and Gibbs energy are written as below:

$$H \equiv U + PV \quad (2.5)$$

$$G \equiv H - TS \quad (2.6)$$

When equation (2.4) is replaced by equation (2.5):

$$d(nH) = T d(nS) + (nV) dP \quad (2.7)$$

Also similar style combination of (2.6) and (2.7) gives:

$$d(nG) = (nV) dP - (nS) dT \quad (2.8)$$

From equation (2.8), derivative of Gibbs energy correspond to P and T are:

$$\left[\frac{\partial(nG)}{\partial P} \right]_{T,n} = nV \quad (2.9)$$

$$\left[\frac{\partial(nG)}{\partial T} \right]_{P,n} = -nS \quad (2.10)$$

Generally in a single-phase Gibbs energy is function of P, T and n then:

$$d(nG) = \left[\frac{\partial(nG)}{\partial P} \right]_{T,n} dP + \left[\frac{\partial(nG)}{\partial T} \right]_{P,n} dT + \sum_i \left[\frac{\partial(nG)}{\partial n_i} \right]_{P,T,n_j} dn_i \quad (2.11)$$

Chemical potential of species i in the mixture is defined as below:

$$\mu_i \equiv \left[\frac{\partial(nG)}{\partial n_i} \right]_{P,T,n_j} \quad (2.12)$$

Finally Gibbs energy equation is:

$$d(nG) = (nV) dP - (nS) dT + \sum_i \mu_i dn_i \quad (2.13)$$

2.1.1 The chemical potential:

In a closed system with two phases in equilibrium, which are open to each other, mass transfer between phases can be existed. Equation (2.13) is implemented to phases give (Smith et al., 2005):

$$d(nG)^V = (nV)^V dP - (nS)^V dT + \sum_i \mu_i^V dn_i^V \quad (2.14)$$

$$d(nG)^L = (nV)^L dP - (nS)^L dT + \sum_i \mu_i^L dn_i^L \quad (2.15)$$

Also a total-system property is equal to sum of all partial properties, and then the sum gives:

$$d(nG) = (nV) dP - (nS) dT + \sum_i \mu_i^V dn_i^V + \sum_i \mu_i^L dn_i^L \quad (2.16)$$

By substituting equation (2.8) in equation (2.16) result is:

$$\sum_i \mu_i^V dn_i^V + \sum_i \mu_i^L dn_i^L = 0 \quad (2.17)$$

Because of mass conservation $dn_i^V = -dn_i^L$ so:

$$\sum_i (\mu_i^V - \mu_i^L) dn_i^V = 0 \quad (2.18)$$

Finally:

$$\mu_i^V = \mu_i^L \quad (2.19)$$

Equation (2.19) is valid for all the systems with multiple phases and for other properties as well:

$$\begin{aligned} T^V &= T^L \\ P^V &= P^L \end{aligned} \quad (2.20)$$

2.1.2 Fugacity and fugacity coefficient:

The concept of fugacity is given as an auxiliary function for chemical potential, since chemical potential does not have a physical equivalent in physical environment. Chemical potential for ideal-gas is (Prausnitz et al., 1998):

$$\mu_i = \mu_i^\circ + RT \ln f_i \quad (2.21)$$

From equation (2.19) all of the phases in equilibrium have same chemical potential then:

$$f_i^V = f_i^L \quad (2.22)$$

So, all phases at the same T and P are in equilibrium when the fugacity of components is the same in all phases. In this case vapor and liquid phases both have the same fugacity, so they are in equilibrium.

In order to have a change from pure state into mixture state, equation (2.21) is written:

$$\mu_i - \mu_i^0 = RT \ln \frac{f_i}{f_i^0} \quad (2.22)$$

Where μ_i^0 and f_i^0 are pure state properties.

For a pure ideal gas, fugacity, pressure as well as fugacity for component i in a mixture and partial pressure are the same. This approach happens when P goes to zero:

$$\frac{f_i}{y_i P} \rightarrow 1 \quad P \rightarrow 0 \quad (2.23)$$

By using equation (2.22) on chemical potential for each phase:

$$\mu_i^V - \mu_i^{0V} = RT \ln \frac{f_i^V}{f_i^{0V}} \quad (2.24)$$

$$\mu_i^L - \mu_i^{0L} = RT \ln \frac{f_i^L}{f_i^{0L}} \quad (2.25)$$

Replacing equation (2.24) and (2.25) in equation (2.19) gives:

$$\mu_i^{0V} + RT \ln \frac{f_i^V}{f_i^{0V}} = \mu_i^{0L} + RT \ln \frac{f_i^L}{f_i^{0L}} \quad (2.26)$$

If both phase have the same standard state then:

$$\mu_i^{0V} = \mu_i^{0L} \quad (2.27)$$

$$f_i^{0V} = f_i^{0L} \quad (2.28)$$

From equation (2.27) and (2.28), new concept for phase equilibrium comes out:

$$f_i^V = f_i^L \quad (2.29)$$

Also, it is possible to write a new equation for both phases:

$$\mu_i^V - \mu_i^L = RT \ln \frac{f_i^V}{f_i^L} \quad (2.26)$$

The dimensionless ratio between the fugacity and the real gas pressure is called fugacity coefficient:

$$\varphi_i = \frac{f_i}{y_i P} \quad (2.27)$$

Then fugacity for vapor phase can be written:

$$f_i^V = y_i \varphi_i^V P \quad (2.28)$$

Fugacity coefficient shows the non-ideality from real state of a mixture. For ideal gas mixture $\varphi_i = 1$.

The fugacity for component i in liquid mixture phase is defined:

$$f_i^L = \gamma_i x_i f_i^{0L} \quad (2.29)$$

Where γ_i is the activity coefficient, which is specified in the next part.

2.1.3 Activity and activity coefficient:

Activity is the ratio between fugacity of species i at the desirable condition over the fugacity of that species in standard condition (Prausnitz et al., 1998):

$$a_i = \frac{f_i}{f_i^0} \quad (2.30)$$

For an ideal solution, Henry's law is applied in order to define the fugacity in the liquid phase:

$$f_i^{0L} = x_i H_i \quad (2.32)$$

Also, activity coefficient is the ratio between activity and mole fraction of species i:

$$\gamma_i = \frac{a_i}{x_i} = \frac{f_i}{x_i H_i} \quad (2.32)$$

An analogy is applied in order to find the Gibbs energy definition from the chemical potential concept:

$$G_i = G_i^\circ + RT \ln f_i \quad (2.33)$$

Relation between partial excess Gibbs energy and fugacity is written based on equation (2.22):

$$G_{i(real)} - G_{i(ideal)} = RT \ln \frac{f_{i(real)}}{f_{i(ideal)}} \quad (2.34)$$

Partial excess Gibbs energy is defined:

$$G_i^E = G_{i(real)} - G_{i(ideal)} \quad (2.35)$$

By substituting equation (2.32) in excess Gibbs energy definition:

$$G_i^E = RT \ln \gamma_i \quad (2.36)$$

Total partial excess Gibbs energy for a mixture can be written:

$$G^E = RT \sum x_i \ln \gamma_i \quad (2.37)$$

2.1.4 $\varphi - \varphi$ Method:

This method can be used for ideal vapor-liquid equilibrium which means that both vapor and liquid phase are using fugacity coefficient. Thus, vapor-liquid equilibrium can be written:

$$y_i \varphi_i^V P = x_i \varphi_i^L P \quad (2.38)$$

2.1.5 $\gamma - \varphi$ Method:

Improved Raoult's law contains the activity coefficient to calculate non-idealities in liquid phase. Activity coefficient is introduced for non-ideal liquid, and then vapor-liquid equilibrium can be written (Smith et al., 2005):

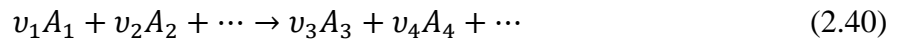
$$y_i \varphi_i^V P = x_i \varphi_i^{sat} P_i^{sat} \gamma_i \exp\left[v_i^{sat} \left(\frac{P - P_i^{sat}}{RT}\right)\right] \quad (2.39)$$

The exponential part is the so-called Poynting factor. For low to moderate pressure this term can be omitted.

2.2 Chemical Equilibria:

Chemical equilibria is a state in which there is no tendency to change for both reactants and products in the macroscopic scale.

Chemical reaction is written (Smith et al., 2005):



Where, v_i is a stoichiometric coefficient and A_i shows a chemical formula. Also, v_i has the sign which can be positive for the product and negative for the reactant.

Since the rate of change of total Gibbs energy at constant P and T is zero at the equilibrium state, then:

$$\sum_i v_i \mu_i = 0 \quad (2.41)$$

2.2.1 Chemical equilibria constant:

From equations (2.33), (2.38) and (2.22) (Smith et al., 2005):

$$\sum_i v_i \left[G_i^\circ + RT \ln \frac{f_i}{f_i^0} \right] = 0$$

$$\text{Or} \quad (2.42)$$

$$\ln \prod_i \left(\frac{f_i}{f_i^0} \right)^{v_i} = - \frac{\sum_i v_i G_i^\circ}{RT}$$

Where \prod_i shows the product over all components, Also, equation (2.39) can be written:

$$\prod_i \left(\frac{f_i}{f_i^0} \right)^{v_i} = K \quad (2.43)$$

Where K which is called the equilibrium constant for the reaction, is defined:

$$K = \exp\left(\frac{-\Delta G}{RT}\right)$$

$$\text{Or} \quad (2.44)$$

$$\ln K = \frac{-\Delta G}{RT}$$

2.2.2 Effect of temperature on the equilibrium constant:

Since ΔG^0 and ΔH^0 are changing with the equilibrium temperature, the dependency of ΔG^0 on T is written as follow (Smith et al., 2005):

$$\frac{d(\Delta G^0/RT)}{dT} = \frac{-\Delta H^0}{RT^2} \quad (2.45)$$

By using equation (2.41) in equation (2.42) a correlation comes out which is called Van't Hoff's equation:

$$\frac{d \ln K}{dT} = \frac{-\Delta H^0}{RT^2} \quad (2.46)$$

The equilibrium constant is a function of temperature and it is written(Weiland et al., 1993):

$$\ln K = A + \frac{B}{T} + C \ln T + DT \quad (2.47)$$

Van't Hoff's equation was applied in order to calculate the heat of absorption.

2.3 Heat of absorption:

In this project, the heat of absorption of CO₂ is the amount of heat, which is required to absorb a specified number of CO₂ by amine solution (Kim et al., 2009). It is written:

$$H_{abs} = \sum_i \zeta_i \Delta H_i \quad (2.48)$$

Where ζ_i is the extent of reaction, i which is based on difference in moles number between two steps of loading CO₂ and also can be written $\zeta_i = \Delta n_i / \Delta n_{CO_2}$. Also ΔH_i is heat of reaction i and it can be calculated from Van't hoff equation (2.46).

Because physical absorption of CO₂ from vapor phase to liquid phase exist, Henrys' constant must be used instead of equilibrium constant, then heat of reaction for this case can be calculated:

$$\frac{d \ln H}{dT} = \frac{-\Delta H^0}{RT^2} \quad (2.49)$$

Where the Henry's constant is defined (Carroll et al., 1991):

$$\ln H = -6.8346 + 1.2818 \times 10^4 / T - 3.7668 \times 10^6 / T^2 + 2.997 \times 10^8 / T^3 \quad (2.50)$$

2.4 Electrolyte Non-Random Two-Liquid (eNRTL) model:

Mixture of CO₂ with amine gives ionic components. This system is so-called electrolyte. Because of the ions the thermodynamic properties of the mixture rely on the forces between these ions(Chen et al., 1982). eNRTL method is recognized by the both molecular components and ionic components, which are combined in three ways of interaction force: ion-ion, molecule-molecule and ion-molecule. Also, these forces are characterized by short range and long range interaction effect. Non-electrolyte systems only have the molecule-molecule interaction which has the short-range force. This concept has been used in NRTL model(Renon and Prausnitz, 1968). eNRTL is the modified version of NRTL, which takes other forces into account. The excess Gibbs energy for an electrolyte system from local interaction is written as below (Chen and Song, 2004):

$$\begin{aligned} \frac{G_m^{ex,lc}}{RT} = & \sum_I \sum_m r_m n_I \left(\frac{\sum_j X_j G_{jm} \tau_{jm}}{\sum_k X_k G_{km}} \right) + \sum_I \sum_c z_c r_{c,I} n_I \left(\sum_a Y_a \frac{\sum_j X_j G_{jc,ac} \tau_{jc,ac}}{\sum_k X_k G_{kc,ac}} \right) \\ & + \sum_I \sum_a z_a r_{a,I} n_I \left(\sum_c Y_c \frac{\sum_j X_j G_{jc,ac} \tau_{jc,ac}}{\sum_k X_k G_{kc,ac}} \right) \end{aligned} \quad (2.51)$$

Also,

$$X_j = C_j x_j, \quad j = c \text{ (cationic), } a \text{ (anionic), } m \text{ (molecule)} \quad (2.52)$$

$$x_j = \frac{\sum_I x_j r_{j,I}}{\sum_I \sum_i x_i r_{i,I}}$$

Where I and J are the component index, n_I is the mole number, $C_j = z_i$ (charge number) for ionic species and $C_j = 1$ for molecular species. x_j and x_j are mole fraction and the segment-based(segment is a framework to indicate the interaction of ion with hydrophilic segment of organic solvents) mole fraction of species j, respectively. $r_{m,I}$, $r_{c,I}$ and $r_{a,I}$ are number of molecular, cationic and anionic segments respectively. Moreover, the anionic charge composition fraction Y_a and the cationic charge composition fraction, Y_c are written:

$$Y_a = \frac{X_a}{\sum_{a'} X_{a'}} \quad (2.53)$$

$$Y_c = \frac{X_c}{\sum_{c'} X_{c'}} \quad (2.54)$$

Three types of adjustable binary model parameters are available in the same way of interaction with binary forces. Also, the model contains: the symmetric nonrandom factor parameters α , and the asymmetric binary interaction energy parameters τ and they are written as below:

$$\alpha_{mm'} = \alpha_{m'm} \quad \alpha_{m,ca} = \alpha_{ca,m} \quad \alpha_{ca,ca'} = \alpha_{ca',ca} \quad \alpha_{ca,c'a} = \alpha_{c'a,ca} \quad (2.55)$$

$$\tau_{mm'} = \tau_{m'm} \quad \tau_{m,ca} = \tau_{ca,m} \quad \tau_{ca,ca'} = \tau_{ca',ca} \quad \tau_{ca,c'a} = \tau_{c'a,ca} \quad (2.56)$$

The model adjustable binary parameters give an average mixing rule in order to calculate α_{cm} and α_{am} :

$$\alpha_{cm} = \sum_a Y_a \alpha_{m,ca} \quad (2.57)$$

$$\alpha_{am} = \sum_c Y_c \alpha_{m,ca} \quad (2.58)$$

Also, the rule below can be used to calculate G_{cm} (Gibbs energy-cationic segment) and G_{am} (Gibbs energy-anionic segment):

$$G_{cm} = \sum_a Y_a G_{ca,m} \quad (2.59)$$

$$G_{am} = \sum_c Y_c G_{ca,m} \quad (2.60)$$

Then binary parameters τ_{cm} and τ_{am} are written:

$$\tau_{cm} = -\frac{\ln G_{cm}}{\alpha_{cm}} \quad (2.61)$$

$$\tau_{am} = -\frac{\ln G_{am}}{\alpha_{am}} \quad (2.62)$$

Finally local activity coefficient for species i can be written:

$$\begin{aligned}
\ln \gamma_m^{lc} = & \frac{\sum_j X_j G_{jm} \tau_{jm}}{\sum_K X_k G_{km}} + \sum_{m'} \frac{X_{m'} G_{mm'}}{\sum_K X_k G_{km'}} \left(\tau_{mm'} - \frac{\sum_k X_k G_{km'} \tau_{km'}}{\sum_K X_k G_{km'}} \right) \\
& + \sum_c \sum_a \frac{Y_a X_c G_{mc,ac}}{\sum_K X_k G_{ka,ac}} \left(\tau_{mc,ac} - \frac{\sum_k X_k G_{kc,ac} \tau_{kc,ac}}{\sum_K X_k G_{kc,ac}} \right) \\
& + \sum_a \sum_c \frac{Y_c X_a G_{ma,ac}}{\sum_K X_k G_{ka,ac}} \left(\tau_{mc,ac} - \frac{\sum_k X_k G_{ka,ca} \tau_{ka,ca}}{\sum_K X_k G_{ka,ca}} \right)
\end{aligned} \tag{2.63}$$

$$\begin{aligned}
\frac{1}{z_c} \ln \gamma_c^{lc} = & \sum_a Y_a \frac{\sum_j X_k G_{kc,ac} \tau_{kc,ac}}{\sum_K X_k G_{kc,ac}} + \sum_m \frac{X_m G_{cm}}{\sum_K X_k G_{km}} \left(\tau_{cm} - \frac{\sum_k X_k G_{km} \tau_{km}}{\sum_K X_k G_{km}} \right) \\
& + \sum_a \sum_{c'} \frac{Y_{c'} X_a G_{ca,c'a}}{\sum_K X_k G_{ka,c'a}} \left(\tau_{ca,c'a} - \frac{\sum_k X_k G_{kc,c'a} \tau_{kc,c'a}}{\sum_K X_k G_{kc,c'a}} \right)
\end{aligned} \tag{2.64}$$

$$\begin{aligned}
\frac{1}{z_a} \ln \gamma_a^{lc} = & \sum_c Y_c \frac{\sum_j X_k G_{kc,ac} \tau_{kc,ac}}{\sum_K X_k G_{kc,ac}} + \sum_m \frac{X_m G_{am}}{\sum_K X_k G_{km}} \left(\tau_{am} - \frac{\sum_k X_k G_{km} \tau_{km}}{\sum_K X_k G_{km}} \right) \\
& + \sum_a \sum_{c'} \frac{Y_{a'} X_c G_{ca,c'a}}{\sum_K X_k G_{ka,c'a}} \left(\tau_{ca,c'a} - \frac{\sum_k X_k G_{kc,c'a} \tau_{kc,c'a}}{\sum_K X_k G_{kc,c'a}} \right)
\end{aligned} \tag{2.65}$$

eNRTL model had been used in Diego's code to find the correct activity coefficient for liquid phase.

3. Modeling of reaction calorimeter:

In this chapter, brief introduction about apparatus which was modeled and detail descriptions about the logic behind the model are presented. Programming parts were coded with MATLAB. The main challenge in this project which took long time was to figure out the procedure to develop a model since there was not any step by step procedure to guide the coding. Also, debugging the code was time consuming.

3.1 Reaction calorimeter apparatus:

This equipment consist of several parts such as reaction colorimeter which has 2000 cm³ capacity, CO₂ gas cylinder, CO₂ mass flow controller, amine solution feed bottle and vacuum pump. Apparatus is shown in Figure 3.1.

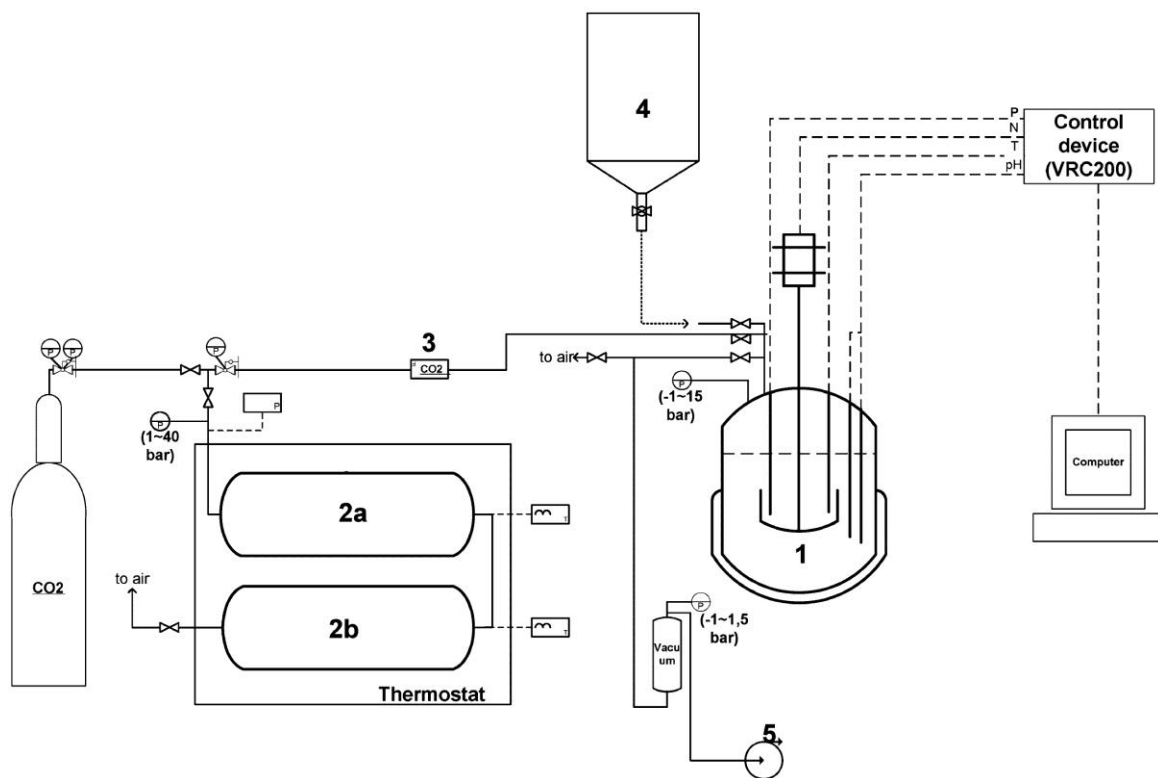


Figure3.1: Vapor-liquid equilibrium apparatus(Kim, 2009)

First, pressure inside the reaction calorimeter is decreased by the vacuum pump in order to have a correct estimation of partial pressure of components. Then, desired amount of amine solution which is measured with the scale, is added to the reactor. After that, CO₂ is loaded to the reactor and the amount of CO₂ is shown by the mass flow meter. The pressure and the temperature in the reactor is measured simultaneously with the heat flow, in order to compensate for the heat of absorption. The data is logged with a computer. Finally the experimental results are shown in the computer. In addition a cooling system is used to control the temperature of the reactor(Kim, 2009).

After each experiment, amine solution is drained from the reactor, then the reactor is washed by water and an inert gas like N₂ should be used to dry the reactor in order to prepare the reactor for the next experiment.

3.2 Code development:

The logics behind the codes are the most important issue since the program will be developed based on it. Since the logics are based on the thermodynamic rules, the final results must be reasonable from thermodynamic point of view.

This project has been divided into two main parts, loading calculation and calculation of heat of absorption.

3.2.1 Loading calculation:

Loading is the number of moles of loaded CO₂ divided by the number of amine's moles. This equation is written as follow:

$$\alpha = \frac{n_{loaded\ co2-liquid}}{n_{amine-liquid}} \quad (3.1)$$

As an assumption all the CO₂ was injected to the liquid phase at the first step. Loading calculation is an iterative process which needs an initial loading. In order to calculate the initial loading, first step at the beginning is:

$$n_{CO2-liquid} = n_{CO2-injected} \quad (3.2)$$

Also, Mass of the amine solution can be measured by a scale before pouring it inside the reactor. So this is a known parameter. The solvent solution consists of amine and water, so the concentration of amine is known as well. Temperature is given, since one of the goals is to find a respond against each given temperature.

Number of amine's moles can be calculated as follow:

$$n_{MEA} = \frac{MEA\ concentration \times Mass\ of\ amine\ solution}{MW_{MEA}} \quad (3.3)$$

After finding the number of moles for MEA, initial loading can be calculated from equation (3.1).

In-house code which can calculate the vapor-liquid equilibrium has some inputs and outputs. The inputs are: Temperature, loading and MEA concentration and the outputs are: partial pressure of components in vapor phase, mole fraction of components in liquid phase and activity coefficient.

By giving the temperature, MEA concentration and initial loading, partial pressure of components in vapor phase and mole fraction of components in liquid phase can be calculated by the code.

Base on the assumption, entire moles of CO₂ are going to the liquid phase at the first step (No CO₂ presents in vapor phase at the first step). Then the objective of the code is to find the amount of CO₂, which goes to the vapor phase in the other steps so for calculating this amount, volume of the vapor phase is required. Procedure can be started from liquid phase since the volume of the reactor is known and based on assumptions, volume of solution can be calculated. Then the difference of between total volume and liquid phase volume gives the volume of gas phase. This procedure can be seen as below:

$$V_{liquid} = \frac{m_{liquid}}{\rho_{loaded}} \quad (3.4)$$

m_{liquid} is sum of the m_{CO_2} , m_{MEA} and m_{water} in the liquid phase and for the first step mass of the solution can be substitute for the mass of the MEA and Water. ρ_{loaded} is determined by a model for loaded CO₂ in MEA solution. This model is written separately as a function which has some input and outputs. The inputs are: Temperature, MEA's mole fraction, mole fraction of water and loading and the outputs are: loaded density and unloaded density. This part of the code is written in "roardi.m" (appendix A). The unloaded density and loaded density is calculated using the model of Hartono et al.2013 (Hartono et al., 2013):

$$\rho_{unloaded} = \frac{x_1 MW_1 + x_2 MW_2}{V^E + \frac{x_1 MW_1 + x_2 MW_2}{\rho_1 + \rho_2}} \quad (3.6)$$

1 and 2 are representative of MEA and water, respectively. V^E is the excess molar volume and it is written:

$$V^E = (-1.9210 + 1.6738 \times 10^{-3} \times T - 3.0951 x_1 + 3.4412 x_1^2)x_1(1 - x_1) \quad (3.7)$$

The density of MEA and water can be calculated:

$$\rho_{MEA} = -5.3270 \times 10^{-7} \times T^2 - 7.4762 \times 10^{-4} \times T + 1.0308 \quad (3.8)$$

$$\rho_{water} = -2.5598 \times 10^{-6} \times T^2 - 1.9691 \times 10^{-4} \times T + 1.004 \quad (3.9)$$

$$\rho_{loaded} = \frac{\rho_{unloaded}}{1 - w_{CO2 loaded}(1 - \phi^3)} \quad (3.10)$$

$$w_{CO2 loaded} = \frac{\alpha x_1 m_{CO2}}{x_1 m_1 + (1 - x_1 - \alpha x_1) m_2 + \alpha x_1 m_{CO2}} \quad (3.11)$$

Where ϕ represents the volume expansion and it is written:

$$\phi = \frac{k_1 x_1 \alpha + k_2 x_1}{k_3 + x_1} \quad (3.12)$$

$$k_1 = 0.29 \pm 0.05 \quad k_2 = 0.18 \pm 0.02 \quad k_3 = 0.66 \pm 0.03$$

From calculations, loaded density and mass of the liquid phase, volume of the liquid phase can be computed. Then the difference of total volume and liquid phase's volume gives:

$$V_{vapor} = V_{total} - V_{liquid} \quad (3.13)$$

The total volume represents the volume of the reactor which is 2 liter.

The next step is to find the mass of species in the vapor phase. The ideal gas law is used to calculate the total concentration of vapor phase but in order to apply it to the real gas model; compressibility factor z , is applied. Compressibility factor is computed from Peng-Rabinson equation which is used in Diego's code in order to find the fugacity coefficient in the vapor phase. The procedure can be written as:

$$C_T = \frac{P_T}{z R T} \quad (3.14)$$

P_T can be computed from partial pressure of the species:

$$P_T = \sum_i P_i \quad (3.15)$$

Also, mole fraction in the vapor phase can be written:

$$y_i = \frac{P_i}{P_T} \quad (3.16)$$

After finding C_T , total number of moles in the vapor phase can be calculated:

$$n_T = C_T \cdot V_{vapor} \quad (3.17)$$

Then by obtaining n_T , mass of the components in the vapor phase is written:

$$m_i = n_T \cdot y_i \cdot MW_i \quad (3.18)$$

By using equation (3.18), mass of the MEA, water and CO₂ in the vapor phase are calculated. Then the difference of the initial value for mass of the components in liquid phase and computed values for vapor phase, gives the new value for mass of the components which remain in the liquid phase:

$$m_{i \text{ excess}} = m_{i \text{ liquid}} - m_{i \text{ vapor}} \quad (3.19)$$

Then new calculation for loading is:

$$\alpha_{new} = \frac{m_{CO_2 \text{ excess}}/MW_{CO_2}}{m_{MEA \text{ excess}}/MW_{MEA}} \quad (3.20)$$

For adjusting loading, this procedure should be written in a loop in order to optimize the response. Condition must be provided for the loop in order to converge to a desirable answer:

$$error = \alpha_{new} - \alpha_{old} \quad (3.21)$$

Also, tolerance is introduced to have a limit for the error. Iteration process remains till the loop can satisfy the tolerance. This procedure is written in “reactorm.m” (Appendix A). This code is written as a function which takes mass of solution, moles of CO₂ in each loading, MEA concentration and temperature as the input and returns total pressure, partial pressure of components, new loading and mole matrix which comes further to calculate heat of absorption. The main code is written in “recorder.m” (Appendix A). All the amounts of CO₂

(CO₂ moles) which are added step by step in to the reactor, are written as a vector and main file takes each of these steps and send them into “reactor.m” file in order to find a new loading, total pressure and partial pressure of CO₂ in vapor phase. Finally, new loadings are plotted against the total pressures as well as partial pressures of CO₂ for entire steps of loading. Figure 3.2 indicates simple flow chart of loading calculation procedure.

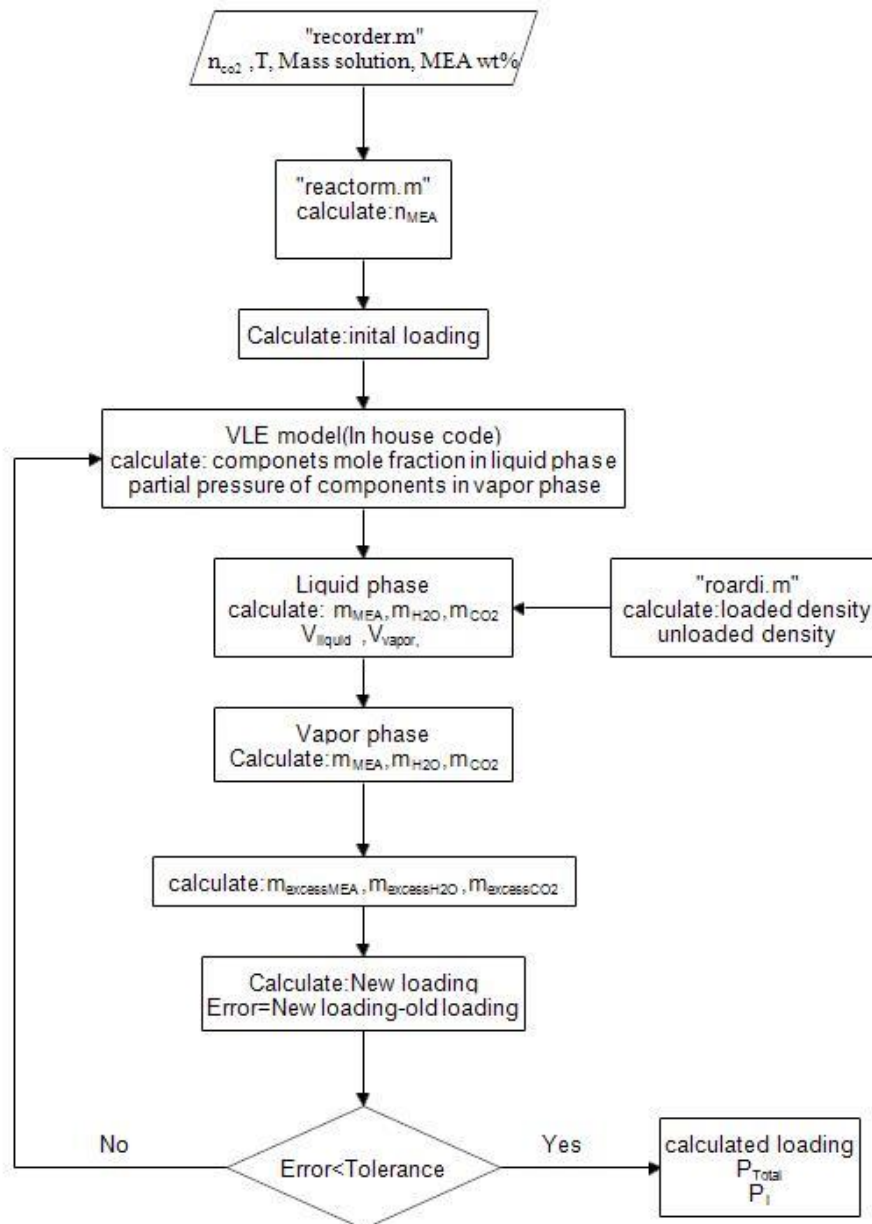


Figure 3.2: Loading calculation procedure

3.2.2 Heat of absorption:

Heat of absorption can be calculated from equation (2.48).

$$H_{abs} = \sum_i \zeta_i \Delta H_i$$

In order to use this equation, extent of reaction ζ_i , is required for each reaction. Correct key component should be selected for each reaction. Key component is the component which is involved only once in the reaction package. The key components for equation (1.1) till (1.6) are written in Table 3.1:

Table 3.1: Key components

Reaction name	Reaction	Key component
Dissociation of water	$2H_2O \rightleftharpoons H_3O^+ + OH^-$	OH^-
Dissociation of carbon dioxide	$2H_2O + CO_2 \rightleftharpoons H_3O^+ + HCO_3^-$	HCO_3^-
Dissociation of bicarbonate	$H_2O + HCO_3^- \rightleftharpoons H_3O^+ + CO_3^{2-}$	CO_3^{2-}
Dissociation of protonatedamine	$H_2O + RNH_3^+ \rightleftharpoons H_3O^+ + RNH_2$	RNH_3^+
Carbamate reversion to bicarbonate	$H_2O + RNHCOO^- \rightleftharpoons RNH_2 + HCO_3^-$	$RNHCOO^-$
Physical dissolution of carbon dioxide	$CO_2(gas) \rightleftharpoons CO_2(liquid)$	CO_2

Extent of reaction ζ_i , is calculated from the difference in the number of moles between the final and initial value based on key components for each reaction, divided by the number of CO_2 moles. Table 3.2 indicates difference of the moles for key components.

Table 3.2: Difference of the moles for each equation based on their key component

Reaction	$\Delta n_{key\ component}$
$2H_2O \rightleftharpoons H_3O^+ + OH^-$	$n_{f\ OH^-} - n_{i\ OH^-}$
$2H_2O + CO_2 \rightleftharpoons H_3O^+ + HCO_3^-$	$(n_{f\ HCO_3^-} - n_{i\ HCO_3^-}) - (n_{f\ CO_3^{2-}} - n_{i\ CO_3^{2-}})$ $+ (n_{f\ RNHCOO^-} - n_{i\ RNHCOO^-})$
$H_2O + HCO_3^- \rightleftharpoons H_3O^+ + CO_3^{2-}$	$n_{f\ CO_3^{2-}} - n_{i\ CO_3^{2-}}$
$H_2O + RNH_3^+ \rightleftharpoons H_3O^+ + RNH_2$	$n_{f\ RNH_3^+} - n_{i\ RNH_3^+}$
$H_2O + RNHCOO^- \rightleftharpoons RNH_2 + HCO_3^-$	$n_{f\ RNHCOO^-} - n_{i\ RNHCOO^-}$
$CO_2(gas) \rightleftharpoons CO_2(liquid)$	$(n_{f\ CO_2} - n_{i\ CO_2}) + (n_{f\ HCO_3^-} - n_{i\ HCO_3^-})$ $- (n_{f\ CO_3^{2-}} - n_{i\ CO_3^{2-}})$ $+ (n_{f\ RNHCOO^-} - n_{i\ RNHCOO^-})$

By applying equation (2.46) which is so-called Van't Hoff's equation, enthalpy of each equation can be calculated:

$$\Delta H_i^0 = R T^2 \frac{dK}{dT} \quad (3.22)$$

Also, derivation of equation (2.47) respects to temperature is written:

$$\frac{dK}{dT} = \frac{-B}{T^2} + \frac{C}{T} + D \quad (3.23)$$

Where B, C and D are the constants which are written in the in-house code from Diego Pinto. Also, he found this coefficient from Hessen et al. 2010 (Hessen et al., 2010).

Instead of the physical absorption of CO₂, equation (3.22) can be used for the rest of the reactions.

For the last reaction, Henry's constant is used. Derivative of equation (2.50) respects to temperature is:

$$\frac{dH}{dt} = -1.2818 \times 10^4 / T^2 - 2 \times 3.7668 \times 10^6 / T^3 - 3 \times 2.997 \times 10^8 / T^4 \quad (3.24)$$

Finally heat of absorption can be calculated based on equation (2.48).

This procedure is written in "heatabs.m" (Appendix A). The inputs of this file are: Mole matrix which shows the moles of key components for entire loading steps, total number of loading and Temperature. It returns heat of absorption and related-heat of the each reaction. This file is called by the main code "recorder.m" and heat of absorption is plotted vs. loading. Simple flow chart of heat of absorption's programming procedure can be seen in Figure 3.3.

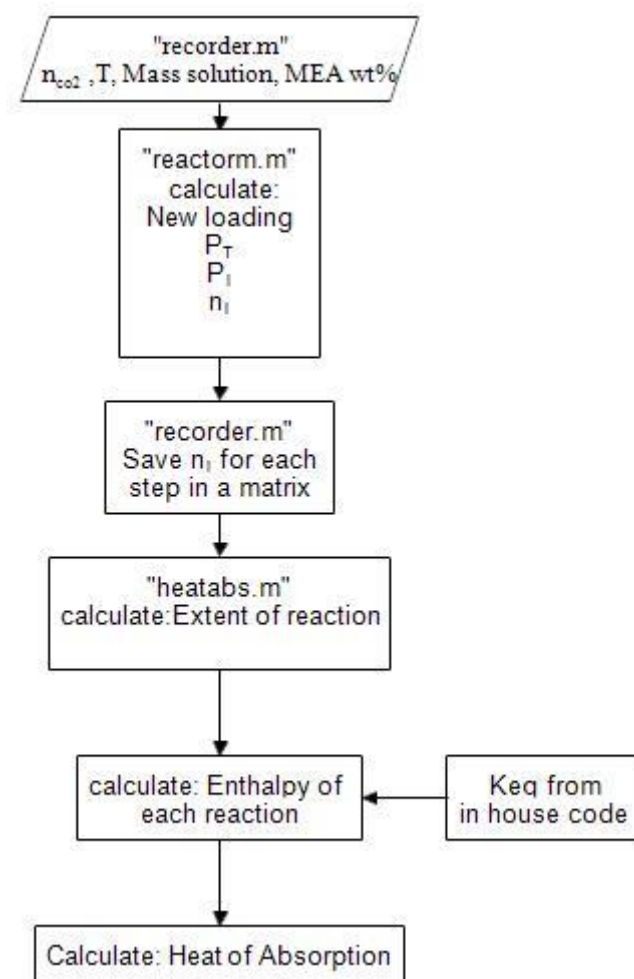


Figure 3.3: Heat of absorption's programming procedure

4. Results and Discussion:

Results of this project are presented in this chapter alongside the relative discussions.

4.1 Vapor-liquid equilibrium model verification:

The in-house vapor-liquid equilibrium model was validated before being used. Experimental data from Aronu et al.(Aronu et al., 2011) are used to validate the model. Same loadings are applied in both model and experimental data. Figure 4.1 shows total pressure of the model and experimental data for 30% MEA solution at 40 °C and 80 °C.

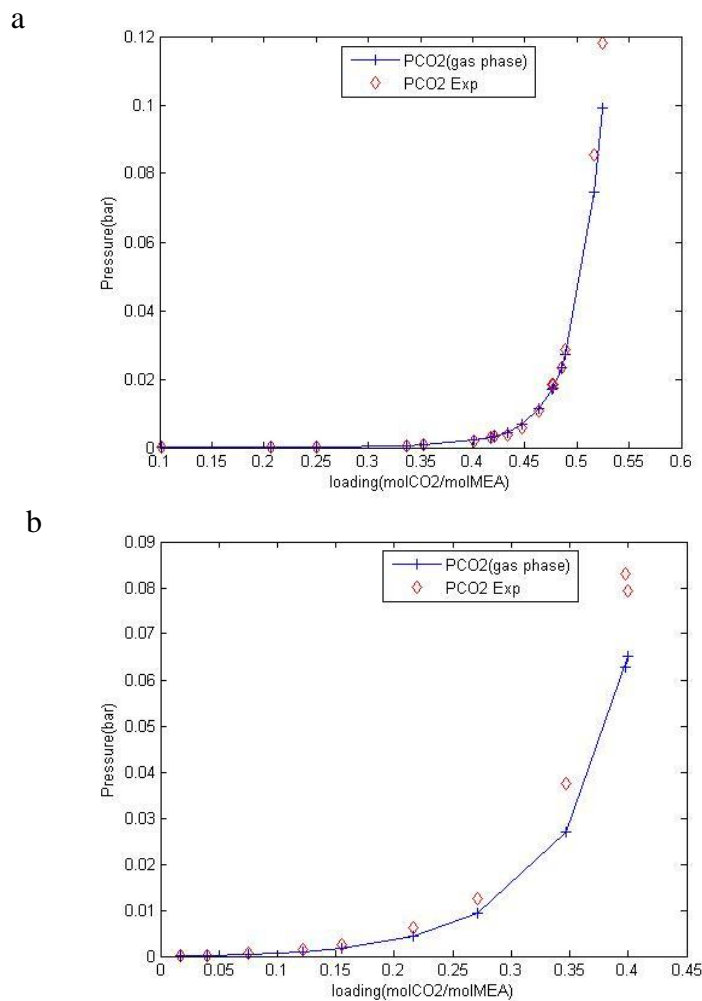


Figure 4.1: P_{CO_2} for the model and experimental data -30% MEA, 40C° (a), 80C° (b)

As it can be seen in Figure 4.1 modeled and experimental data shows the same trend for partial pressure of, however model shows slightly under prediction value of P_{CO_2} for the loadings higher than 0.5 and 0.25 at 40 °C and 80 °C, respectively. Although, the maximum under prediction of the VLE model is approximately 16% (at loading 0.52) at 40°C and 25% (at loading 0.35) at 80 °C. Additionally, P_{CO_2} almost remains stable for the loadings lower than 0.45 at 40 °C (a) and after that, it increases sharply. At 80 °C (b) partial pressure of CO_2 increases slowly at loadings below 0.15 . Then P_{CO_2} increases gradually for the loadings between 0.15 and 0.35, after that there is a rapid rise in P_{CO_2} for the loadings more than 0.35. Total pressure in gas phases increases by increasing the temperature and because of this reason total pressure changes faster at 80 °C compare to total pressure at 40 °C.

The same comparison is done for the total pressure above loaded 30% MEA solution at 120 °C. Figure 4.2 shows total pressure for both model and experimental data from Aronu et al.(Aronu et al., 2011).

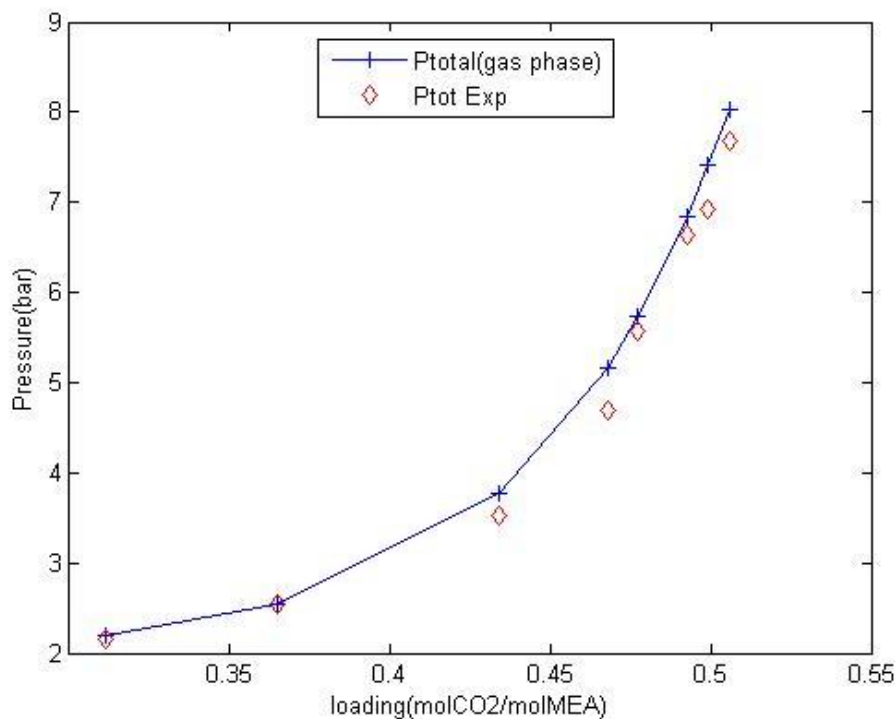


Figure 4.2: P_{Total} for the model and experimental data-30% MEA at 120 C°

As it can be seen in Figure 4.2, total pressure for both model and experimental data has the same trend, although VLE model has a small over prediction for the loadings higher than 0.43 and the maximum over prediction is around 9 % (at loading 0.46). Since vapor-liquid model has minor error compare to the experimental data, it is applied in this project.

4.2 Loading calculation:

The aim of loading calculation is to find the correct properties in both vapor and liquid phases. Experimental data from Inna Kim (Appendix B) are used to check the accuracy of the written code to calculate the loading.

Reactor is dried by N_2 after each cleaning then remaining inert gas creates small pressure inside the reactor. In addition, there is no term to consider the pressure creation because of the inert gas inside the written code for loading calculation, thus after comparison of the total pressure from the model and experimental data, difference between the values is added to the total pressure in the code as an initial pressure. Figure 4.2 shows the two cases for each state, with and without initial pressure.

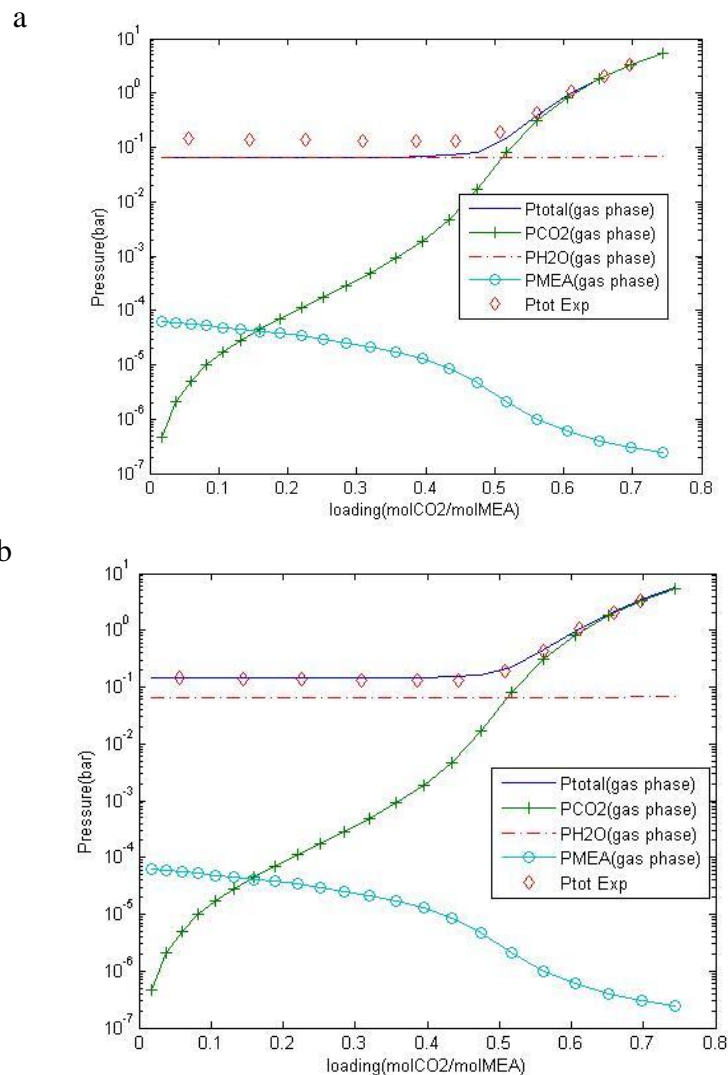


Figure 4.2: Without initial pressure (a), with initial pressure (b)-MEA 30%, 40 C°

As it can be seen in Figure 4.2 (a), there is a small difference between blue curve (Total pressure from written model) and diamond-shaped red points (Total pressure from experimental data). According to Figure 4.2(a), this difference in pressure is around 0.08 bar , also reactor is evacuated to -0.95~-1 barg in experiment before adding CO₂ so 0.08 bar is fairly close to the actual pressure in experiment and this amount which is added to the total pressure as an initial pressure in the code.

Figure 4.3, 4.4 and 4.5 show pressure vs. loading from model and experimental data.

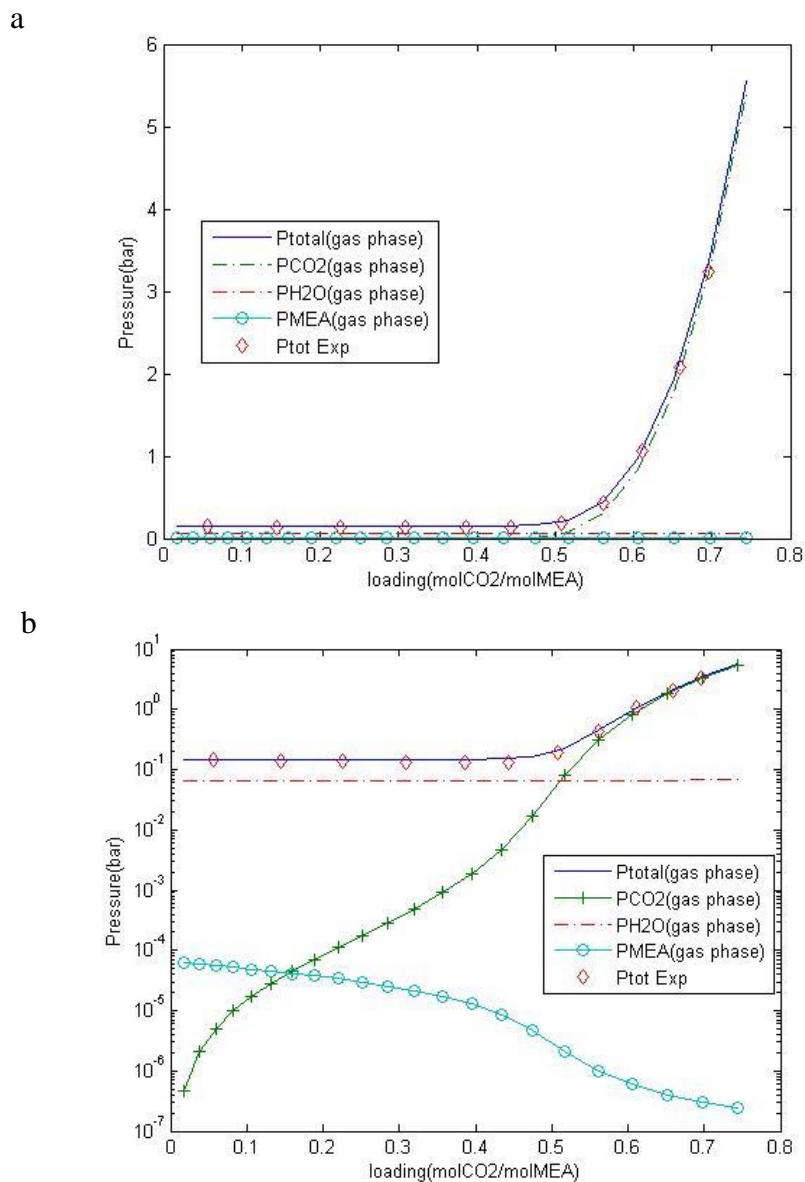


Figure 4.3: Loading calculation-Pressure vs. Loading-30% MEA, 40 C° –normal scale (a) and semi-logarithmic scale (b)

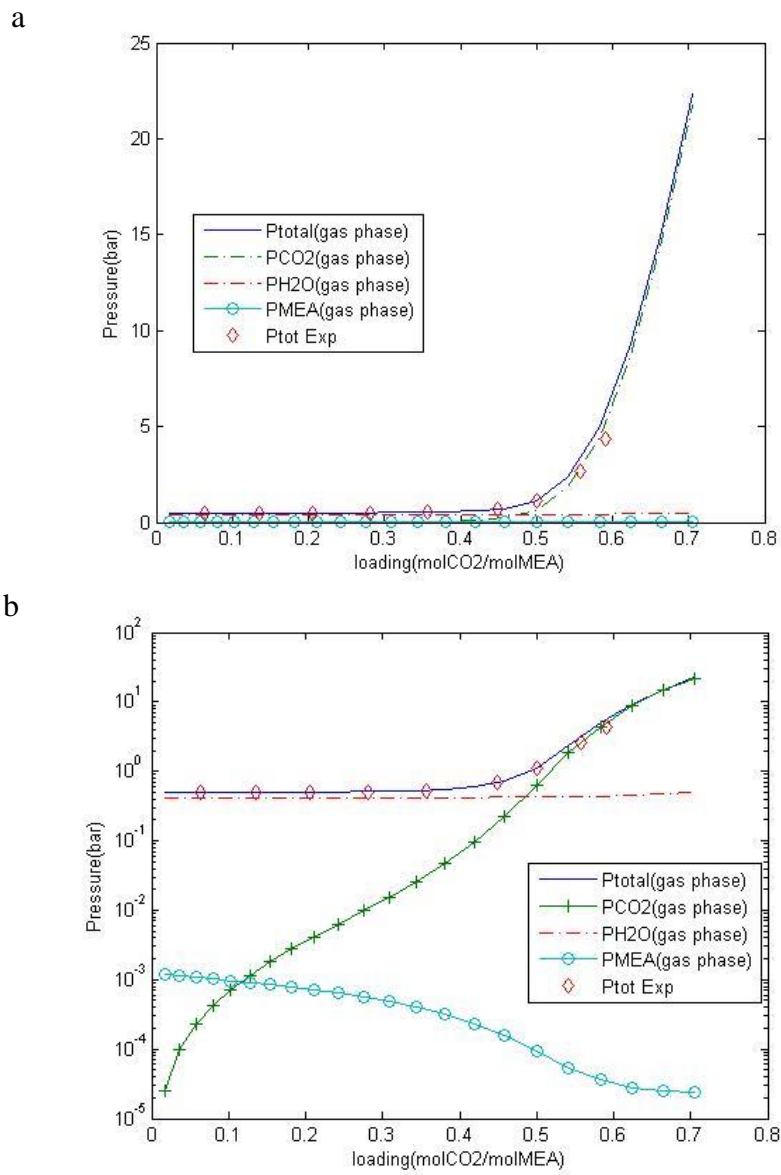


Figure 4.4: Loading calculation-Pressure vs. Loading-30% MEA, 80 C° –normal scale (a) and semi-logarithmic scale (b)

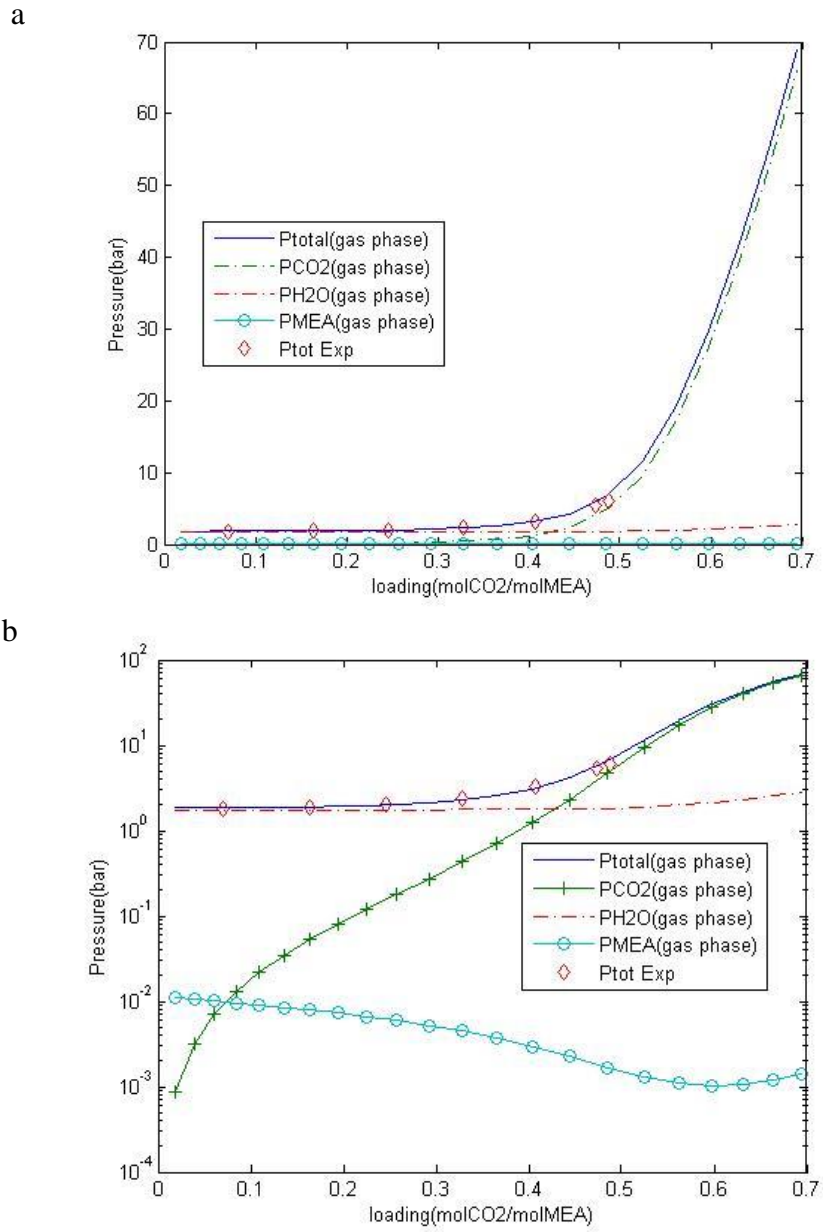


Figure 4.5: Loading calculation-Pressure vs. Loading-30% MEA, 120 C^o –normal scale (a) and semi-logarithmic scale (b)

As it can be seen in Figure 4.2, 4.3 and 4.4, total pressure in both model and experimental data remain stable for loadings less than 0.5, 0.45 and 0.4 at 40 °C, 80 °C and 120 °C, respectively. For loadings higher than these values, total pressure increases rapidly for both model and experimental data. Higher loading means that the number of mole of CO₂ increases for the specific amount of the solvent solution (MEA + Water), thus the solvent is not able to absorb more CO₂ and the extra amount of CO₂ which goes to vapor phase. Furthermore, higher temperature decreases the ability of solvent to absorb more CO₂, since the vapor pressures of the components in gas phase (H₂O, CO₂, MEA) are rising by increase the temperature. For total pressure both the model and experimental data have the same trend, although model shows small over prediction compared to the experimental data.

4.3 Heat of absorption:

Experimental data for heat of absorption from Kim and Svendsen (Kim and Svendsen, 2007) are used to compare them with calculated heat of absorption. In addition, written model to calculate heat of absorption is compared to model of Kim et al. (Kim et al., 2009). The same programming procedure for calculating heat of absorption is used for both models (written model in this work and model of Kim et al.), although instead of equilibrium constant equation, specific equations for calculating enthalpy of reactions are taken from Inna Kim in-house code. The model of Kim is written in “heat.m” (Appendix A) to compare heat of absorption model in this project with her model. Figure 4.6 indicates heat of absorption vs. average loading at 40 °C, 80 °C and 120 °C for the two different models. Since extend of reaction ($\frac{\Delta n_{key\ component}}{\Delta n_{CO_2\ total}}$) is calculated between two loading steps, mean average of these two steps of loading must be used in order to plot the result.

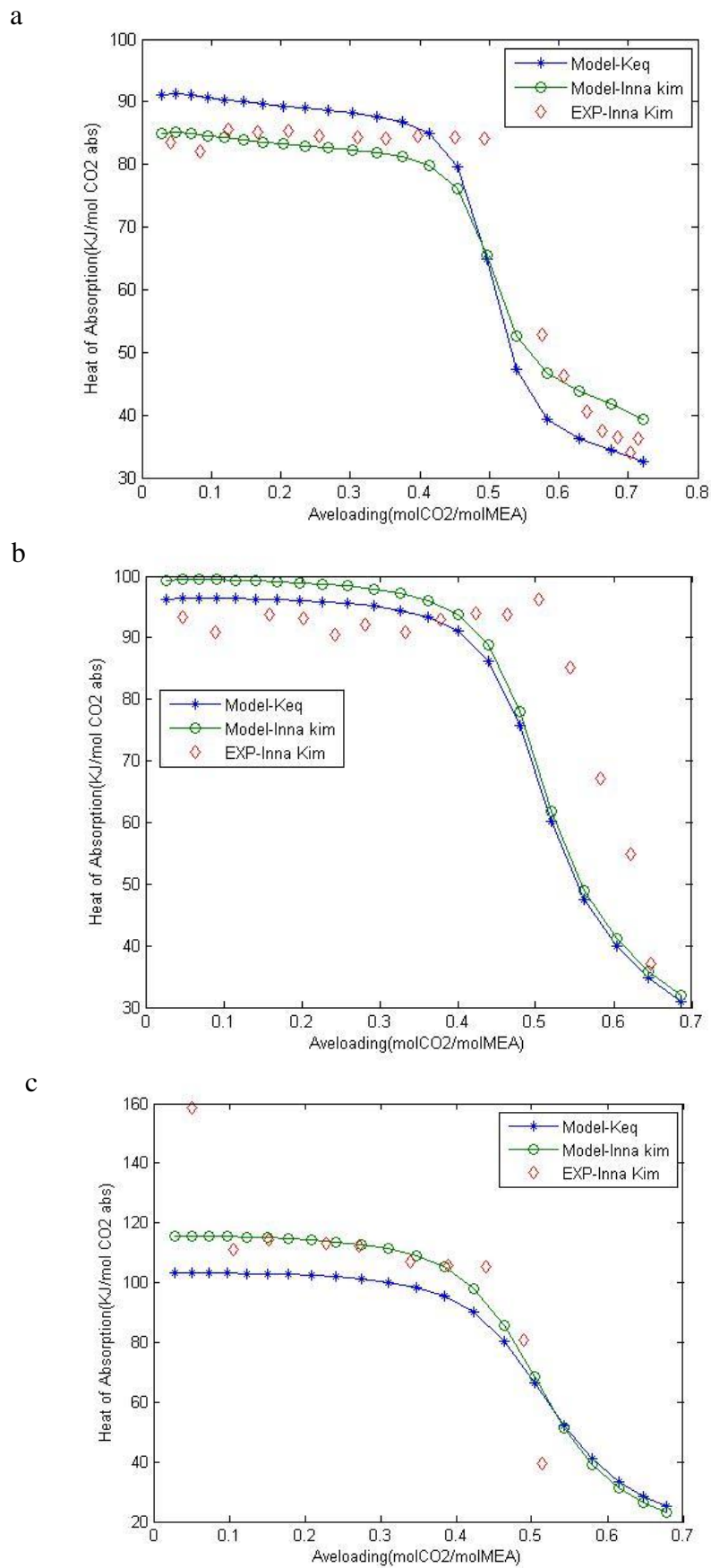


Figure 4.6: Heat of absorption-30% MEA-40C° (a), 80C° (b), 120C°(c)

As it can be seen in Figure 4.6 total heat of absorption for two models and experimental data has the same trend. At 40 °C, model which is based on equilibrium constant (keq) has a small over prediction for loadings less than 0.4 compare to the experimental data, however Kim et al. model(Kim et al., 2009) shows a small under prediction for the same range of loadings. At 80 °C both models have over prediction compared to the experimental data but Kim et al. model(Kim et al., 2009)has a higher over prediction for the loadings less than 0.4. For 120 °C, Kim et al. model(Kim et al., 2009)fits with the experimental data but the keq-model has a slight under prediction for the loadings smaller than 0.4. For these three temperatures, heat of absorption drops for loadings higher than 0.4 in models and experimental data, but it falls sharply at 40 °C and 80 °C compare to 120 °C. There is an under prediction for keq-model and Inna's model at 40 °C and 80 °C and 120 °C for loadings between 0.4-0.6.

General overview of Figure 4.6 shows that total heat of absorption for both models almost stays stable for the loadings less than 0.4 and eventually it decreases for loadings higher than 0.4 for all temperatures.

In order to find the difference between the models based on the equilibrium constants and Inna's model for heat of absorption, enthalpies of all reactions are plotted. Figure 4.7, 4.8 and 4.9 demonstrate the heat of each reaction at 40 °C, 80 °C and 120 °C, respectively.

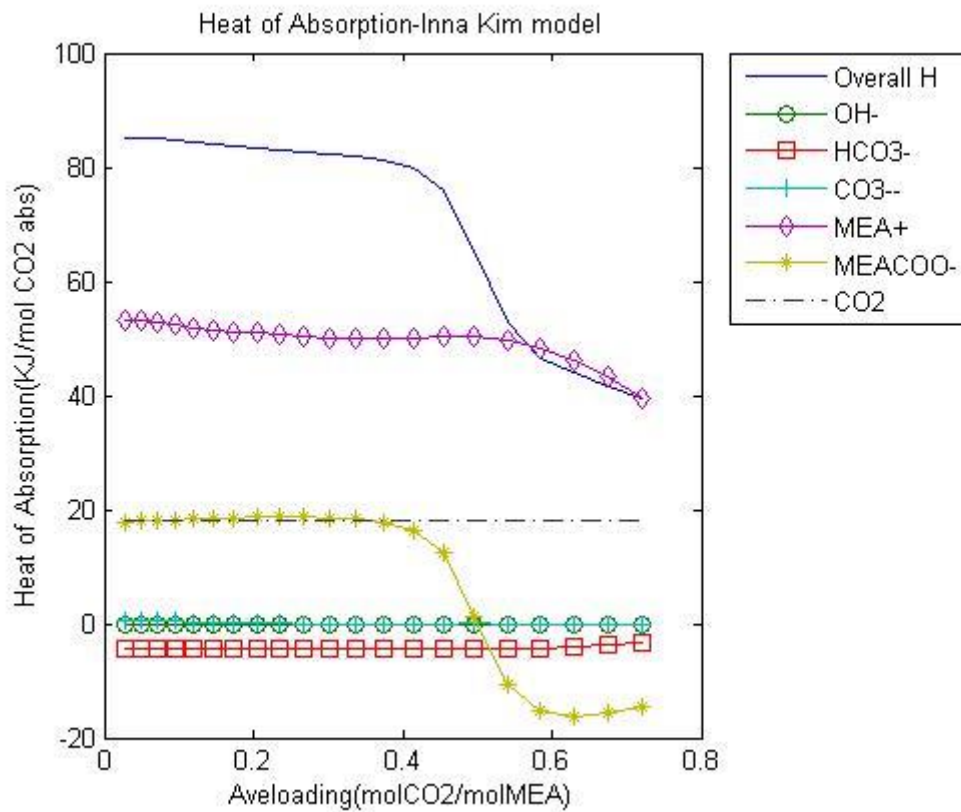
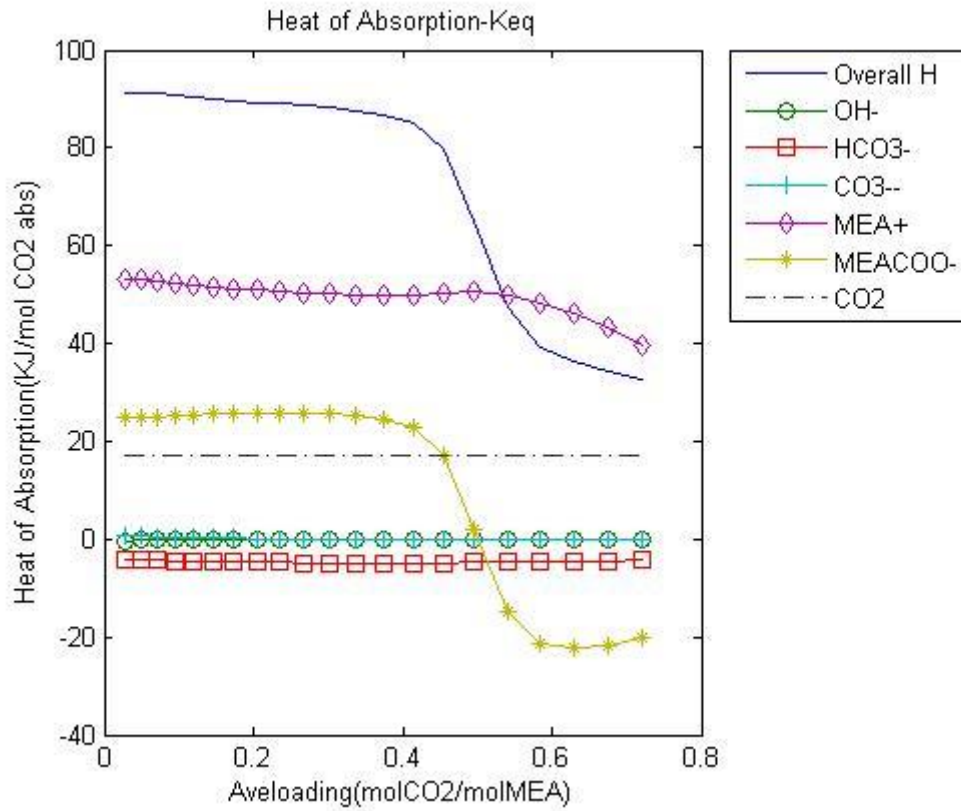


Figure 4.7: Heat of each reaction-30% MEA at 40 C°, Keq-model and Kim et al.

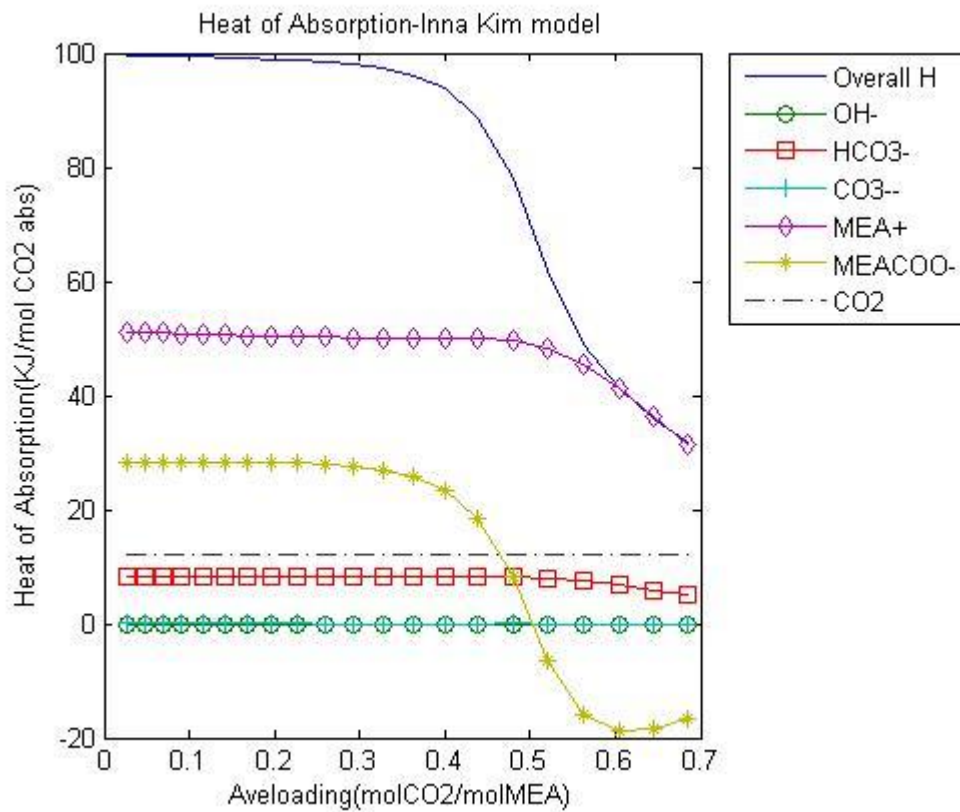
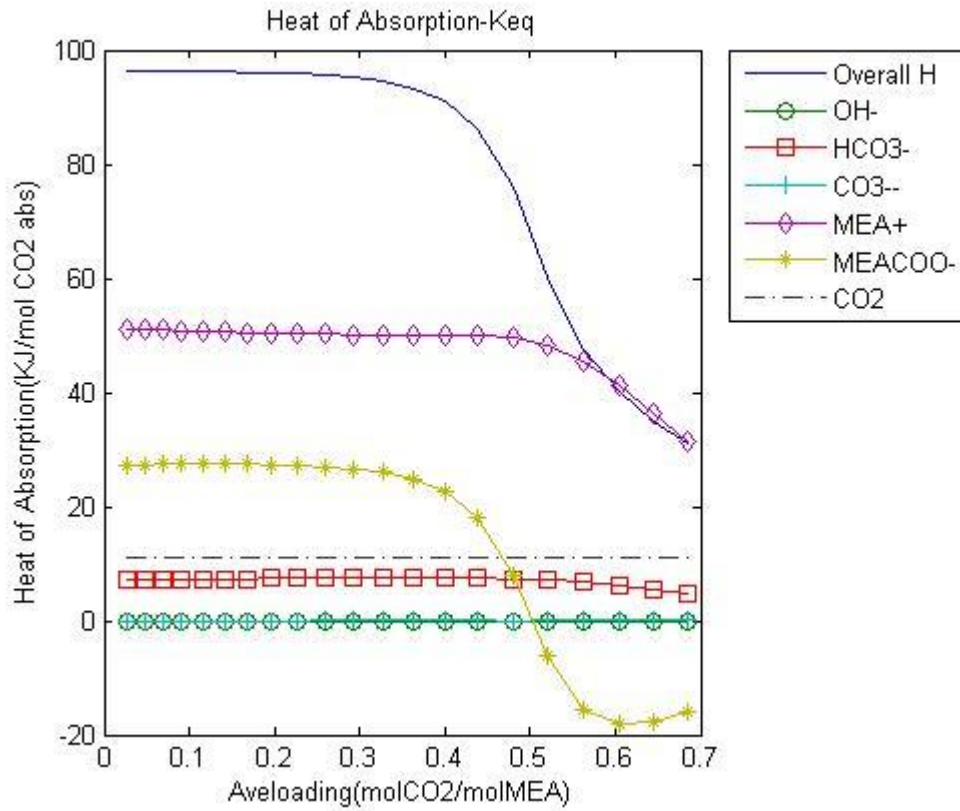


Figure 4.8: Heat of each reaction-30% MEA at 80 C°, Keq-model and Kim et al.

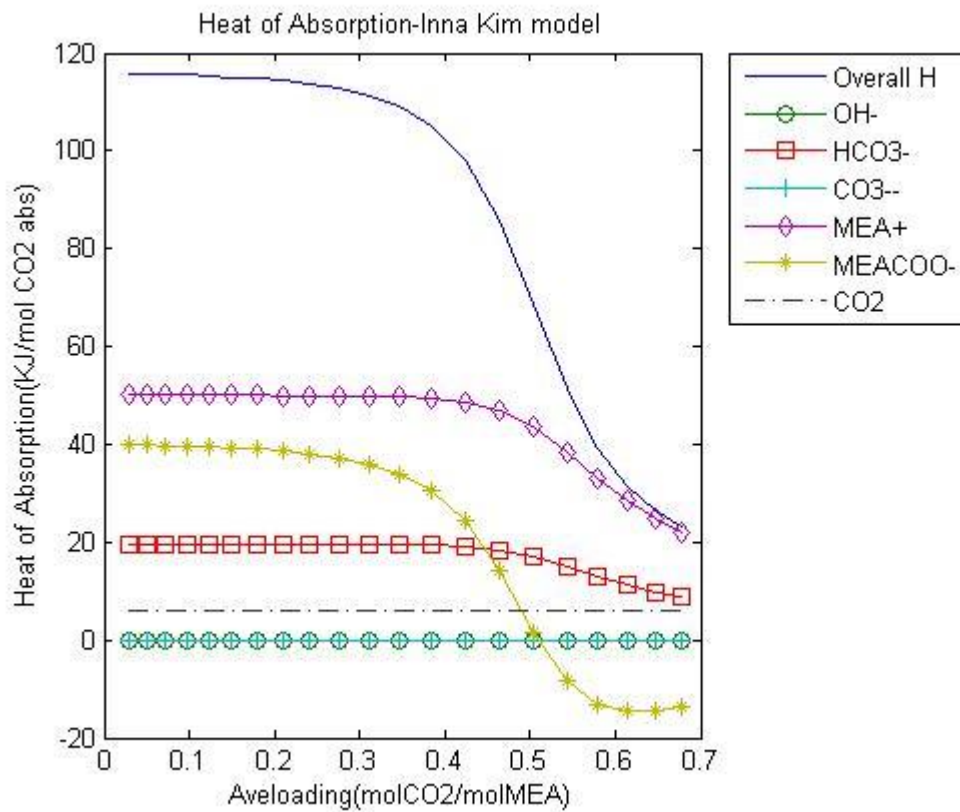
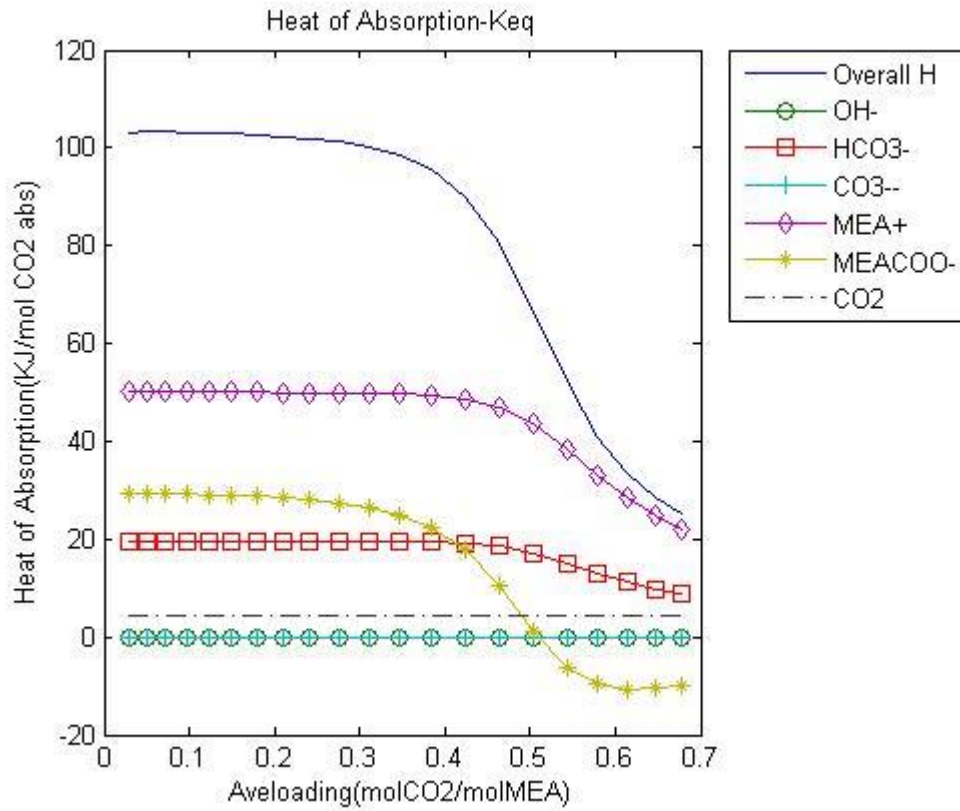


Figure 4.9: Heat of each reaction-30% MEA at 40 C°, Keq-model and Kim et al.

As it can be seen in Figure 4.7, 4.8 and 4.9 Kim et al. model (Kim et al., 2009) has higher heat of absorption compare to the keq-model for the loadings less than 0.4 at 40 °C but for the other temperatures it is vice versa at the same range of loadings. H_{MEACOO^-} (equation (1.5)) is the only difference in both models and it is the factor which causes the difference in total heat of absorption between these two models. Since extent of reaction is the same for both models then these two models have a different value for enthalpy of reaction (1.5). The reason is the different equations which are used in calculation of enthalpy of reaction (1.5). The rest of the reactions almost have the same value for heat in the both models.

5. Conclusion:

The aim of this project was to model the reaction calorimeter in order to calculate the heat of absorption which is the most important parameter in this work. Project was divided to several parts in order to make the programming procedure simpler. Vapor-liquid verification was the first part which was implemented to validate the in-house codes of Diego Pinto which is based on the vapor-liquid thermodynamic and the comparison between the vapor-liquid model and experimental data determined that the model can be used for the rest of the project. Also, comparison of total pressure and heat of absorption calculated from the written model in this project and experimental data for 30% MEA solvent at 40 °C, 80 °C and 120 °C indicate acceptable results based on the thermodynamic theory and the modeling procedure. Since all of the results from the model almost cover the experimental data, this written model might be good to describe the reaction calorimeter in order to meet the goal of this project.

5.1 Future work:

There are some aspects which can be considered in the future works:

- Better programming procedure for calculation of the loadings.
- Find other methods to calculate the overall heat of absorption and compare it with written model in this project. For example, use Partial pressure of CO_2 instead of equilibrium constant in Van't Hoff's equation
- Find more experimental data for heat of absorption for MEA

Bibliography:

- ARONU, U. E., GONDAL, S., HESSEN, E. T., HAUG-WARBERG, T., HARTONO, A., HOFF, K. A. & SVENDSEN, H. F. 2011. Solubility of CO₂ in 15, 30, 45 and 60 mass% MEA from 40 to 120° C and model representation using the extended UNIQUAC framework. *Chemical engineering science*, 66, 6393-6406.
- AUSTGEN, D. M., ROCHELLE, G. T., PENG, X. & CHEN, C. C. 1989. Model of vapor-liquid equilibria for aqueous acid gas-alkanolamine systems using the electrolyte-NRTL equation. *Industrial & Engineering Chemistry Research*, 28, 1060-1073.
- BIROL, F. 2004. World energy outlook. Paris, France: International Energy Agency, 2008: 13.
- CARROLL, J. J., SLUPSKY, J. D. & MATHER, A. E. 1991. The solubility of carbon dioxide in water at low pressure. *Journal of Physical and Chemical Reference Data*, 20, 1201-1209.
- CHEN, C. C., BRITT, H., BOSTON, J. & EVANS, L. 1982. Local composition model for excess Gibbs energy of electrolyte systems. Part I: Single solvent, single completely dissociated electrolyte systems. *AIChE Journal*, 28, 588-596.
- CHEN, C. C. & SONG, Y. 2004. Generalized electrolyte-NRTL model for mixed-solvent electrolyte systems. *AIChE journal*, 50, 1928-1941.
- GLUYAS, J. & MATHIAS, S. 2013. *Geological storage of carbon dioxide (CO₂): Geoscience, technologies, environmental aspects and legal frameworks*, Elsevier.
- HARTONO, A., MBA, E. O. & SVENDSEN, H. F. 2013. Prediction of N₂ O Solubility in Alkanolamine Solutions from the Excess Volume Property. *Energy Procedia*, 37, 1744-1750.

- HESSEN, E. T., HAUG-WARBERG, T. & SVENDSEN, H. F. 2010. The refined e-NRTL model applied to CO₂-H₂O-alkanolamine systems. *Chemical Engineering Science*, 65, 3638-3648.
- KANNICHE, M., GROS-BONNIVARD, R., JAUD, P., VALLE-MARCOS, J., AMANN, J.-M. & BOUALLOU, C. 2010. Pre-combustion, post-combustion and oxy-combustion in thermal power plant for CO₂ capture. *Applied Thermal Engineering*, 30, 53-62.
- KIM, I. 2009. Heat of reaction and VLE of post combustion CO₂ absorbents. *Ph.D. Thesis. Norwegian University of Science and Technology: Trondheim, Norway.*
- KIM, I., HOFF, K. A., HESSEN, E. T., HAUG-WARBERG, T. & SVENDSEN, H. F. 2009. Enthalpy of absorption of CO₂ with alkanolamine solutions predicted from reaction equilibrium constants. *Chemical Engineering Science*, 64, 2027-2038.
- KIM, I. & SVENDSEN, H. F. 2007. Heat of absorption of carbon dioxide (CO₂) in monoethanolamine (MEA) and 2-(aminoethyl) ethanolamine (AEEA) solutions. *Industrial & engineering chemistry research*, 46, 5803-5809.
- KOHL, A. L. & NIELSEN, R. 1997. *Gas purification*, Gulf Professional Publishing.
- METZ, B., DAVIDSON, O., DE CONINCK, H., LOOS, M. & MEYER, L. 2005. IPCC, 2005: IPCC special report on carbon dioxide capture and storage. Prepared by Working Group III of the Intergovernmental Panel on Climate Change. *Cambridge, United Kingdom and New York, NY, USA, 442 pp.*
- OKI, Y., INUMARU, J., HARA, S., KOBAYASHI, M., WATANABE, H., UMEMOTO, S. & MAKINO, H. 2011. Development of oxy-fuel IGCC system with CO₂ recirculation for CO₂ capture. *Energy Procedia*, 4, 1066-1073.

- PRAUSNITZ, J. M., LICHTENTHALER, R. N. & DE AZEVEDO, E. G. 1998. *Molecular thermodynamics of fluid-phase equilibria*, Pearson Education.
- RENON, H. & PRAUSNITZ, J. M. 1968. Local compositions in thermodynamic excess functions for liquid mixtures. *AIChE journal*, 14, 135-144.
- SKOVHOLT, O. 1993. CO₂ transportation system. *Energy Conversion and Management*, 34, 1095-1103.
- SMITH, J. M., VAN NESS, H. C. & ABBOTT, M. M. 2005. *Introduction to chemical engineering thermodynamics*, Boston: McGraw-Hill; 7th ed.
- TOBIESEN A.F 2006. Modelling and experimental study of carbon dioxide absorption and desorption. Ph.D. *Ph.D. Thesis. Norwegian University of Science and Technology: Trondheim, Norway*, pp. 138.
- WANG, M., LAWAL, A., STEPHENSON, P., SIDDEERS, J. & RAMSHAW, C. 2011. Post-combustion CO₂ capture with chemical absorption: A state-of-the-art review. *Chemical Engineering Research and Design*, 89, 1609-1624.
- WEILAND, R. H., CHAKRAVARTY, T. & MATHER, A. E. 1993. Solubility of carbon dioxide and hydrogen sulfide in aqueous alkanolamines. *Industrial & engineering chemistry research*, 32, 1419-1430.

Appendix A:

recorder.m

Main file which the all of the sub-files are connected to this file.

```
clc
clear all
close all

innae% Inna's experimental data
%%%%%%%%%%%%%%%%%%%%%%%%%%%%%%%%%%%%%%%%%%%%%%%%%%%%%%%%%%%%%%%%%%%%%%%%%MEA data%%%%%%%%%%%%%%%%%%%%%%%%%%%%%%%%%%%%%%%%%%%%%%%%%%%%%%%%%%%%%%%%%%%%%%%%%
%For each Temperature(40,80,120), related numbers(40,80,120) must be      %
%changed for MEA data in the same way                                     %
%%%%%%%%%%%%%%%%%%%%%%%%%%%%%%%%%%%%%%%%%%%%%%%%%%%%%%%%%%%%%%%%%%%%%%%%%
MEAconcentration=.3;% wt MEA
T=40;% C
T1=T;
msolution=msolution_40;%gr MEA+water
moleco2=0.12:.01:.33;%given CO2 moles
moleco2_1=moleco2_40;%moleco2-experimental
Ptot_exp=Ptot_40;
innahoa%Inna's experimental data-Heat of absorption
HOA=heat_40(:,2);
loadingh=heat_40(:,1);
%%%%%%%%%%%%%%%%%%%%%%%%%%%%%%%%%%%%%%%%%%%%%%%%%%%%%%%%%%%%%%%%%%%%%%%%%Calculate loading%%%%%%%%%%%%%%%%%%%%%%%%%%%%%%%%%%%%%%%%%%%%%%%%%%%%%%%%%%%%%%%%%%%%%%%%%
n=length(moleco2);
Moleco2=zeros(n,1);
Moleco2(1)=moleco2(1);

for i=2:n
    Moleco2(i)=Moleco2(i-1)+moleco2(i);
end

for i=1:n
    [Ptot(i) Pco2(i) Ph2o(i) Pmea(i) cloading(i)
nmole]=reactorm(msolution,Moleco2(i),MEAconcentration,T);
    molematrix(:,i)=nmole;
end

for i=2:n
```

```

    avecloading(i-1)=(cloading(i-1)+cloading(i))/2;
end
T=T+273
%%%%%%%%%%%%%%%%%%%%%%%%%%%%%%%%%%%%%%%%%%%%%%%%%%%%%%%%%%%%%%%%%%%%%%%%Heat of Absorption%%%%%%%%%%%%%%%%%%%%%%%%%%%%%%%%%%%%%%%%%%%%%%%%%%%%%%%%%%%%%%%%%%%%%%%%
[H,HH]=heat(molematrix,n,T);
[Hd,HHd]=heatabs(molematrix,n,T);

%%%%%%%%%%%%%%%%%%%%%%%%%%%%%%%%%%%%%%%%%%%%%%%%%%%%%%%%%%%%%%%%%%%%%%%%

Ptot=(Ptot./100)+0.08;%0.08 for vacuum
Pco2=Pco2./100;
Ph2o=Ph2o./100;
Pmea=Pmea./100;

%%%%%%%%%%%%%%%%%%%%%%%%%%%%%%%%%%%%%%%%%%%%%%%%%%%%%%%%%%%%%%%%%%%%%%%%Calculate loading based on experimental data%%%%%%%%%%%%%%%%%%%%%%%%%%%%%%%%%%%%%%%%%%%%%%%%%%%%%%%%%%%%%%%%%%%%%%%%

moleco2=moleco2_1;
Moleco2_1(1)=moleco2_1(1);
n=length(moleco2_1);

for i=2:n
    Moleco2_1(i)=Moleco2_1(i-1)+moleco2_1(i);
end
for i=1:n
    [Ptot_1(i) Pco2_1(i) Ph2o_1(i) Pmea_1(i) cloading_1(i)
nmole_1]=reactorm(msolution,Moleco2_1(i),MEAconcentration,T1);
end
%%%%%%%%%%%%%%%%%%%%%%%%%%%%%%%%%%%%%%%%%%%%%%%%%%%%%%%%%%%%%%%%%%%%%%%%

figure(1)
plot(cloading,Ptot,cloading,Pco2,'-.',cloading,Ph2o,'-.',cloading,Pmea,'-
o')
hold on
plot(cloading_1,Ptot_exp,'rd')
ylabel('Pressure(bar)')
xlabel('loading(molCO2/molMEA)')
legend('Ptotal(gas phase)','PCO2(gas phase)','PH2O(gas phase)','PMEA(gas
phase)','Ptot Exp')

```

```

legend('location','best')

figure(2)
semilogy(cloading,Ptot,cloading,Pco2,'-+',cloading,Ph2o,'-
.',cloading,Pmea,'-o')
hold on
semilogy(cloading_1,Ptot_exp,'rd')
ylabel('Pressure(bar)')
xlabel('loading(molCO2/molMEA)')
legend('Ptotal(gas phase)','PCO2(gas phase)','PH2O(gas phase)','PMEA(gas
phase)','Ptot Exp')
legend('location','best')

figure(3)
plot(avecloading,HHd,'-*',avecloading,HH,'-o',loadingh,HOA,'d')
ylabel('Heat of Absorption(KJ/mol CO2 abs)')
xlabel('Aveloading(molCO2/molMEA)')
legend('Model-Keq','Model-Inna kim','EXP-Inna Kim')

figure(4)
plot(avecloading,HHd,avecloading,Hd(1,:),'-o',avecloading,Hd(2,:),'-
s',avecloading,Hd(3,:),'-+',avecloading,Hd(4,:),'-d',avecloading,Hd(5,:),'-
*',avecloading,Hd(6,:),'-.')
ylabel('Heat of Absorption(KJ/mol CO2 abs)')
xlabel('Aveloading(molCO2/molMEA)')
legend('Overall H','OH-','HCO3-','CO3--','MEA+','MEACOO-','CO2')
legend('location','bestoutside')
title('Heat of Absorption-Keq')

figure(5)
plot(avecloading,HH,avecloading,H(1,:),'-o',avecloading,H(2,:),'-
s',avecloading,H(3,:),'-+',avecloading,H(4,:),'-d',avecloading,H(5,:),'-
*',avecloading,H(6,:),'-.')
ylabel('Heat of Absorption(KJ/mol CO2 abs)')
xlabel('Aveloading(molCO2/molMEA)')
legend('Overall H','OH-','HCO3-','CO3--','MEA+','MEACOO-','CO2')
legend('location','bestoutside')
title('Heat of Absorption-Inna Kim model')

```


reactor.m

Calculates new loading.

Input: Mass solution, number of CO₂ moles, MEA concentration, temperature

Output: Total pressure, P_{CO₂}, P_{MEA}, P_{H₂O}, new loading, mole fraction in liquid phase

```
function [Ptot Pco2 Ph2o Pmea cloading
nmole]=reactorm(msolution,moleco2,MEAconcentration,T)
%%%%%%%%%%%%%%%%%%%%%%%%%%%%%%%%%%%%%%%%%%%%%%%%%%%%%%%%%%%%%%%%%%%%%%%%%%%%%%Input%%%%%%%%%%%%%%%%%%%%%%%%%%%%%%%%%%%%%%%%%%%%%%%%%%%%%%%%%%%%%%%%%%%%%%%%%%%%%%
% msolution=1;%gr MEA+water
% loading=0.4;% molco2/molMEa
% MEAconcentration=.8;% wt MEA
% T=40;% C
Vtotal=2;%liter
constant
%%%%%%%%%%%%%%%%%%%%%%%%%%%%%%%%%%%%%%%%%%%%%%%%%%%%%%%%%%%%%%%%%%%%%%%%%%%%%%Initial Loading%%%%%%%%%%%%%%%%%%%%%%%%%%%%%%%%%%%%%%%%%%%%%%%%%%%%%%%%%%%%%%%%%%%%%%%%%%%%%%
xmea=MEAconcentration;%wt MEA
mmea=xmea*msolution;%mass MEA gr
molemea=mmea/61.08;
loading=moleco2/molemea;
%%%%%%%%%%%%%%%%%%%%%%%%%%%%%%%%%%%%%%%%%%%%%%%%%%%%%%%%%%%%%%%%%%%%%%%%%%%%%%
tol=1e-5;
maxstep=10;
step=1;
error=1;
%%%%%%%%%%%%%%%%%%%%%%%%%%%%%%%%%%%%%%%%%%%%%%%%%%%%%%%%%%%%%%%%%%%%%%%%%%%%%%inital step%%%%%%%%%%%%%%%%%%%%%%%%%%%%%%%%%%%%%%%%%%%%%%%%%%%%%%%%%%%%%%%%%%%%%%%%%%%%%%
T1=T;

while step<maxstep && tol<error
[pv,nv,gamma]=MEA_NRTL(T1,loading,MEAconcentration);% pv(partial pressure
in gas phase,H2O,CO2,MEA)-nv(mole fraction in liquid phase- gamma eNRTL
properties

%%%%%%%%%%%%%%%%%%%%%%%%%%%%%%%%%%%%%%%%%%%%%%%%%%%%%%%%%%%%%%%%%%%%%%%%%%%%%%Liquid%%%%%%%%%%%%%%%%%%%%%%%%%%%%%%%%%%%%%%%%%%%%%%%%%%%%%%%%%%%%%%%%%%%%%%%%%%%%%%
if step==1%initial step
xmea=MEAconcentration;%wt MEA
xwater=1-xmea;%wt water
mmea=xmea*msolution;%mass MEA gr
mwater=xwater*msolution;%mass MEA gr
```

```

molefmea=(mmea/61.08)/((mmea/61.08)+(mwater/18.01));
molenumberco2=loading*(mmea/61.08);
mco2liq=molenumberco2*44;%mass co2 gr
mmealiq=mmea;
mwaterliq=mwater;
[rounloaded roloaded]=roardi(T1,xmea,xwater,loading);
Vsolution=(msolution+mco2liq)/roloaded)*10^-3; %liter!!!!
Vgas=Vtotal-Vsolution;

```

```
else
```

```

[rounloaded roloaded]=roardi(T1,nv(3),nv(1),loading);

Vsolution=(mco2liq+mmealiq+mwaterliq)/roloaded)*1000; %liter
Vgas=Vtotal-Vsolution;

```

```
end
```

```
%%%%%%%%%%%%%%%%%%%%%%%%%%%%%%%%%%%%%%%%%%%%%%%%%%%%%%%%%%%%%%%%%%%%%%%%Gas%%%%%%%%%%%%%%%%%%%%%%%%%%%%%%%%%%%%%%%%%%%%%%%%%%%%%%%%%%%%%%%%%%%%%%%%
```

```
load('fug.mat')%z from fugcoeff
```

```
T=T+273;
```

```
Ptotalgas=sum(pv);
```

```
y=pv./Ptotalgas;
```

```
C=Ptotalgas/(z*R*T);
```

```
gastotalmol=C*Vgas*1e3;%mol
```

```
mwatergas=gastotalmol*y(1)*18.01;
```

```
mco2gas=gastotalmol*y(2)*44;%gr
```

```
mmeagas=gastotalmol*y(3)*61.08;%gr
```

```
%%%%%%%%%%%%%%%%%%%%%%%%%%%%%%%%%%%%%%%%%%%%%%%%%%%%%%%%%%%%%%%%%%%%%%%%
```

```
mwaterexcess=mwaterliq-mwatergas;
```

```
mco2excess=mco2liq-mco2gas;
```

```
mmeaexcess=mmealiq-mmeagas;
```

```
oldloading=loading;
```

```
loading=(mco2excess/44)/(mmeaexcess/61.08);
```

```
error=loading-oldloading;
```

```
step=step+1;
```

```
mco2liq=mco2excess;
```

```

mmealiq=mmeaexcess;
mwaterliq=mwaterexcess;
T=T1;
end
[pv,nv,gamma]=MEA_NRTL(T1,loading,MEAconcentration);

molwsolution=sum(nv.*molw');
mtot=msolution+mco2liq;
ntot=mtot/molwsolution;
nmole=nv*ntot;
% nmole=nv;
cloading=loading;
Ptot=sum(pv);
Ph2o=pv(1);
Pco2=pv(2);
Pmea=pv(3);
mtotal=mco2liq+mmealiq+mwaterliq+mco2gas+mmeagas+mwatergas;
end

```

roardi.m

Calculates density for the mixture of solvent and CO₂ in liquid phase.

Input: Temperature, mole fraction of MEA in liquid phase, mole fraction of H₂O in liquid phase, loading

Output: loaded density, unloaded density

```
function [rounloaded roloaded]=roardi(T,xmea,xwater,loading)
x1=xmea;%mole(maybe weight) fraction
x2=xwater;

m1=61.08;%Molecular weight MEA
m2=18.01;%Molecular weight Water
m3=44;%Molecular weight CO2
M1=61.08;%Molecular weight MEA
M2=18.01;%Molecular weight Water
k1=0.29;%+-0.05
k2=0.18;%+-0.2
k3=0.66;%+-0.03

rhoamine = -5.3270E-07.*T.^2 - 7.4762E-04.*T+ 1.0308E+00;%given by Ardi
ro1=rhoamine;%gr/cm3
rhowater= -2.5598E-06.*T.^2 - 1.9691E-04.*T+ 1.0040E+00;
ro2=rhowater;%gr/cm3

fi=(k1.*x1.*loading+k2.*x1)./(k3+x1);
wco2=(loading.*x1.*m3)./(x1.*m1+((1-x1-loading.*x1).*m2)+loading.*x1.*m3);

VE=(-1.9210+1.6792e-3.*T-3.0951.*x1+3.4412.*x1^.2).*x1.*x2;%ardi paper

rounloaded=(x1.*M1+x2.*M2)./(VE+((x1.*M1)./ro1)+((x2.*M2)./ro2));
roloaded=rounloaded./(1-wco2.*(1-fi.^3));

end
```

heatabs.m

Calculates heat of absorption based on equilibrium constant.

Input: Mole matrix, length of loading steps, temperature

Output: Overall heat of absorption, heat of each reaction

```
function [H HH]=heatabs(molematrix,n,T)
R=8.314e-3;%KJ/mol.K
for i=2:n
    deltanrx(1,i-1)=molematrix(6,i)-molematrix(6,i-1);%Dissosiation of
water-key component:OH-
    deltanrx(2,i-1)=-molematrix(7,i)+molematrix(7,i-1)+molematrix(8,i)-
molematrix(8,i-1)-molematrix(9,i)+molematrix(9,i-1);%Dissosiation of Carbon
dioxide-key component:HCO3- check the signs!!!!
    deltanrx(3,i-1)=molematrix(8,i)-molematrix(8,i-1);%Dissosiation of
Bicarbonate-key component:CO3--
    deltanrx(4,i-1)=molematrix(5,i)-molematrix(5,i-1);%Dissosiation of
Protonated Amine-key component:MEA+
    deltanrx(5,i-1)=molematrix(9,i)-molematrix(9,i-1);%Carbonate
reversation to bicarbonate-key component:MEACOO-
    deltanrx(6,i-1)=molematrix(2,i)-molematrix(2,i-1)+molematrix(7,i)-
molematrix(7,i-1)+molematrix(8,i)-molematrix(8,i-1)+molematrix(9,i)-
molematrix(9,i-1);%Physical absorption of CO2-Key comonent:CO2
end

% Henry's constant for CO2 [Pa] from Diego's code carol 1991 co2 so

Hr = [-6.8346 1.2814e4 -3.7668e6 2.997e8];
%H = exp(Hr(1) + Hr(2)/T + Hr(3)/(T^2) + Hr(4)/(T^3))*1e6;
dhdt=(-Hr(2)/T^2)-((2*Hr(3))/T^3)-((3*Hr(4))/T^4);%Kpa
%%%%%%%%%%%%%%%%%%%%%%%%%%%%%%%%%%%%%%%%%%%%%%%%%%%%%%%%%%%%%%%%%%%%%%%%

load TER % load equilibrium constants(Keq) from the in house code written
by Diego Pinato
% A B C D for 5 reactions
coeff=keq;
for i=1:6
    if i~=6
        dlndkdt(i)=(-coeff(i,2)/(T^2))+(coeff(i,3)/T)+coeff(i,4);
```

```

deltah(i,1)=R*T^2*dlnkdt(i);
else
    deltax(i,1)=R*T^2*dhdt;
end

end

for i=2:n
    H(1,i-1)=deltah(1)*deltanrx(1,i-1)/deltanrx(6,i-1);
    H(2,i-1)=deltah(2)*deltanrx(2,i-1)/deltanrx(6,i-1);
    H(3,i-1)=deltah(3)*deltanrx(3,i-1)/deltanrx(6,i-1);
    H(4,i-1)=deltah(4)*deltanrx(4,i-1)/deltanrx(6,i-1);
    H(5,i-1)=deltah(5)*deltanrx(5,i-1)/deltanrx(6,i-1);
    H(6,i-1)=deltah(6)*deltanrx(6,i-1)/deltanrx(6,i-1);
end
for i=2:n
    HH(i-1,1)=sum(deltah.*deltanrx(:,i-1))/deltanrx(6,i-1);
end
end

```

heat.m

Calculates heat of absorption based on Inna Kim's model.

Input: Mole matrix, length of loading steps, temperature

Output: Overall heat of absorption, heat of each reaction

```
function [H,HH]=heat(molematrix,n,T)
R=8.314;%KJ/mol.K
for i=2:n
    deltanrx(1,i-1)=molematrix(6,i)-molematrix(6,i-1);%Dissosiation of
water-key component:OH-
    deltanrx(2,i-1)=molematrix(7,i)-molematrix(7,i-1)+molematrix(8,i)-
molematrix(8,i-1)+molematrix(9,i)-molematrix(9,i-1);%Dissosiation of Carbon
dioxide-key component:HCO3- check the signs!!!!
    deltanrx(3,i-1)=molematrix(8,i)-molematrix(8,i-1);%Dissosiation of
Bicarbonate-key component:CO3--
    deltanrx(4,i-1)=molematrix(5,i)-molematrix(5,i-1);%Dissosiation of
Protonated Amine-key component:MEA+
    deltanrx(5,i-1)=molematrix(9,i)-molematrix(9,i-1);%Carbonate
reversation to bicarbonate-key component:MEACOO-
    deltanrx(6,i-1)=molematrix(2,i)-molematrix(2,i-1)+molematrix(7,i)-
molematrix(7,i-1)+molematrix(8,i)-molematrix(8,i-1)+molematrix(9,i)-
molematrix(9,i-1);%Physical absorption of CO2-Key comonent:CO2
end

% Henry's constant for CO2 [Pa] from Diego's code

Hr = [-6.8346 1.2814e4 -3.7668e6 2.997e8];
%H = exp(Hr(1) + Hr(2)/T + Hr(3)/(T^2) + Hr(4)/(T^3))*1e6;
dhdt=(-Hr(2)/T^2)-((2*Hr(3))/T^3)-((3*Hr(4))/T^4)*exp(Hr(1) + Hr(2)/T +
Hr(3)/(T^2) + Hr(4)/(T^3));%Kpa
%%%%%%%%%%%%%%%%%%%%%%%%%%%%%%%%%%%%%%%%%%%%%%%%%%%%%%%%%%%%%%%%%%%%%%%%%%%%%%
%%%!!!
load TER
coeff=num2str(keq);% A B C D for 5 reactions
for i=1:6
    if i~=6
        dlnkdt(i)=(-coeff(i,2)/(T^2))+coeff(i,3)/T+coeff(i,4);
        deltah(i,1)=R*T^2*dlnkdt(i);
```

```

else
    deltah(i,1)=R*T^2*dhdt;
end

end

%%%%%%%%%%%%%%%%%%%%%%%%%%%%%%%%%%%%%%%%%%%%%%%%%%%%%%%%%%%%%%%%%%%%%%%%Equation from In house code from Inna Kim%%%%%%%%%%%%%%%%%%%%%%%%%%%%%%%%%%%%%%%%%%%%%%%%%%%%%%%%%%%%%%%%%%%%%%%%
dHr0(1) = (1/1000)*(-711777+9.54028e07*T.^(-1)+2161.02*T-2.212757*T.^2);
dHr0(2) = (-R/1000)*(17262-67.3414.*T+0.04431786.*T.^2);
dHr0(3) = (R/1000)*(6433.628-2.245836.*T-0.04458435.*T.^2);
dHr0(4) = (R/1000)*(6166.116-0.000985*T.^2);
dHr0(5)=(R/1000)*(1.674734287-13.074152510*T+0.065103560*T.^2);
dHr0(6)=(R/1000)*(8477.711-21.95743*T+0.005780748*T.^2);
deltah(:,1)=dHr0;
%%%%%%%%%%%%%%%%%%%%%%%%%%%%%%%%%%%%%%%%%%%%%%%%%%%%%%%%%%%%%%%%%%%%%%%%%%%%%%%%%%%%%%%%%%%%%%%%%%%%%%%%%%%%%%%%%%%%%%%%%%%%%%%%%%%%%%%%%%%%%%%%%%%%%%%%%%%%%%%%%%%%%%%%%%%%%%%%%%%%%%%%%%%%%%%%%%%%%%%%%%%%%%%%%%%%%%%%%%%%%%%%%%%%%%%%%%%%%%%%%%%%%%%%%%%%%%%%%%%%%%%%%%%%%%%%%%%%%%%%%%%%%%%%
for i=2:n
    H(1,i-1)=deltah(1)*deltanrx(1,i-1)/deltanrx(6,i-1);
    H(2,i-1)=deltah(2)*deltanrx(2,i-1)/deltanrx(6,i-1);
    H(3,i-1)=deltah(3)*deltanrx(3,i-1)/deltanrx(6,i-1);
    H(4,i-1)=deltah(4)*deltanrx(4,i-1)/deltanrx(6,i-1);
    H(5,i-1)=deltah(5)*deltanrx(5,i-1)/deltanrx(6,i-1);
    H(6,i-1)=deltah(6)*deltanrx(6,i-1)/deltanrx(6,i-1);
end
for i=2:n
    HH(i-1,1)=sum(deltah.*deltanrx(:,i-1))/deltanrx(6,i-1);
end
end

```


Appendix B:

In house experimental data from Inna Kim

Table 1: Total pressure-experimental data, 30% MEA at 40 C°

Reactor P (bar)	CO ₂ added (mol)
0.149	0.3658
0.143	0.5871
0.140	0.5348
0.139	0.5388
0.134	0.5075
0.134	0.3706
0.134	0.4258
0.187	0.3522
0.434	0.3435
1.068	0.3204
2.077	0.2569
3.230	0.0000

Table 2: Total pressure-experimental data, 30% MEA at 80 C°

Reactor P (bar)	CO ₂ added (mol)
0.505	0.4350
0.496	0.4823
0.494	0.4746
0.489	0.5148
0.498	0.5124
0.522	0.6272
0.687	0.0000
0.681	0.3543
1.117	0.4108
2.647	0.2368
4.315	0.0000

Table 3: Total pressure-experimental data, 30% MEA at 120 C°

Reactor P (bar)	CO ₂ added (mol)
1.797	0.4507
1.810	0.6003
1.874	0.5237
2.010	0.5245
2.340	0.5075
3.250	0.4384
5.368	0.0937
6.101	0.0000